Stony Brook University

Chronic supplementary dl-alpha tocopheryl acetate stimulates brain accelerated aging: S100B, RAGE and Microglia.

A Dissertation Presented

by

Lynn Ann McGoey

to

The Graduate School

in Partial Fulfillment of the

Requirements for the Degree of

Doctor of Philosophy

in

Biopsychology

Stony Brook University

August 2008

Stony Brook University

The Graduate School

Lynn Ann McGoey

We, the dissertation committee for the above candidate for the

Doctor of Philosophy degree, hereby recommend

acceptance of this dissertation.

Patricia M. Whitaker, Ph.D. - Dissertation Advisor
Professor, Department of Psychology

Hoi-Chung Leung, Ph.D. - Chairperson of Defense
Assistant Professor, Department of Psychology

Dr. Gregory Zelinsky, Ph.D.
Associate Professor, Department of Psychology

Efrain C. Azmitia, Ph.D.
Professor, Department of Biology,
New York University

This dissertation is accepted by the Graduate School

Lawrence Martin
Dean of the Graduate School

Abstract of the Dissertation

Chronic supplementary dl-alpha tocopheryl acetate stimulates brain accelerated aging: S100B, RAGE and Microglia.

by

Lynn Ann McGoey

Doctor of Philosophy

in

Biopsychology

Stony Brook University

2008

S100B is a calcium-binding protein largely produced and released by astroglial cells of the brain to have both neurotoxic and neurotrophic effects. The gene for S100B is found on chromosome 21, and thus the protein is thought to be involved in the neuropathology of Down Syndrome (DS) as well as Alzheimer's disease (AD) given that most DS individuals develop AD at an early age. Levels of S100B are particularly high during development and aging, and heightened levels have been associated with neuroinflammatory induced neuronal damage such as that seen with microglial activation and upregulation of the S100B receptor, RAGE (receptor for advanced glycation endproducts). This study examined the effects of heightened levels of S100B on microglial activation, RAGE immunoreactivity and neuronal damage in the hippocampus of S100B-overexpressing transgenic mice as compared to CD1 controls at 1, 3, 6, and 12 months of age. The dietary effect of the antioxidant dl-alpha tocopheryl acetate

(Vitamin E) was also assessed. Results show that S100B overexpression increases microglial reactivity, RAGE upregulation and neuronal loss as the S100B-overexpressing animals age. Within these mice, Vitamin E significantly increased microglial activation and RAGE reactivity at 5.5 and 10 months of age with significant neuronal loss seen by 10 months of age.

Dedication

I dedicate my dissertation work to my family and friends who have given me their never-ending encouragement and support. A special feeling of gratitude will always be for my husband Kevin, my parents John and Linda, and my brothers John and Michael whose words of support will never be forgotten. My family Charles, Jane and P.J. have always been by my side.

I also dedicate my dissertation to my friends who have supported me through this process, especially Stacy, Sarah and Ariel. Literally by my side through all the madness was Alice Borella. A true friend and my biggest supporter, without her encouragement and technical assistance the work would never have been completed. Lee Shapiro was a friend and assistant in editing my dissertation. His time is greatly appreciated.

Finally I dedicate this work to the faculty of Stony Brook University and New York University including my advisor and mentor, Dr. Patricia Whitaker and members of the dissertation committee including Dr. Hoi-Chung Leung, Dr. Gregory Zelinsky and Dr. Efrain Azmitia. I thank Dr. Whitaker for her endless support and guidance and allowing me to discover my love of science and research. I wish to thank my committee members who were more than generous with their expertise and precious time.

Table of Contents

List of Abbreviations

Aβ……..β-amyloid
AD……Alzheimer's disease
AGE's……...advanced glycation endproducts
ANOVA……analysis of variance
CA……*Cornu Ammonis*
CC……CD1 control animals on control diet
CE……CD1 control animals on Vitamin E supplemented diet
CNS……..central nervous system
DS……Down syndrome
IL1β……interleukin-1β
iNOS……inducible nitric oxide
RAGE……receptor for advanced glycation endproducts
PD ……...Parkinson's disease
SC……S100B-overexpressing animals on control diet
SE ……S100B-overexpressing animals on Vitamin E supplemented diet
TNFα ……tumor necrosis factor-α

List of Tables

List of Figures

Chronic supplementary dl-alpha tocopheryl acetate stimulates brain accelerated aging: S100B, RAGE and Microglia

Introduction

The S100 Family: S100B

S100 proteins, initially discovered in nervous system tissue, are a family of 21 different calcium binding proteins that are widely expressed throughout numerous vertebrate tissue types and are involved in intracellular calcium binding, release and overall maintenance (Moore, 1965). This protein family is of the EF-hand type that occurs as dimers, but when activated by calcium, bind to a variety of other proteins to produce their numerous biological effects both intracellularly, those cells expressing the proteins, as well as extracellularly when the proteins are released (Donato, 2001).

S100B is a 21 kDA member of this S100 calcium-binding protein family that is produced by astroglial cells and released into the neuropil by a variety of factors with particularly high levels of expression during development and aging (Lott & Head, 2001; Portela et al., 2002). The gene for S100B is found at location 21q22.3 of chromosome 21, the obligate region for Down Syndrome (DS). Therefore, the protein is thought to be involved in the neuropathology of DS and Alzheimer's disease (AD) given that most DS individuals develop AD at an early age, potentially through a S100B-mediated neuroinflammatory mechanism (Griffin et al, 1989; Griffin et al, 1998a).

Once released, S100B has varied effects on surrounding cells. In some cases at nanomolar concentrations (10^{-9}), S100B is trophic and promotes differentiation, growth, recovery and survival of neurons (Kligman & Marshak, 1985; Winningham-Major et al., 1989; Selinfreund et al., 1991; Barger et al., 1992; Muller et al., 1993; Yan et al., 1997). In other cases at micromolar concentrations (10^{-6}), S100B can be toxic and lead to cell loss and apoptosis (Mariggio et al., 1994; Shapiro et al., 2004). Extracellular S100B is capable of causing changes in glial cellular morphology and gene expression leading to the production of neurotoxic pro-inflammatory cytokines such as interleukin-1β (IL-1β) and tumor necrosis factor-α (TNFα) (Hu et al., 1996; Hofmann et al., 1999; Hu & Van Eldik, 1999; Huttunen et al., 2000; Petrova et al., 2000; Koppal et al., 2001).

There is controversy over the determinants of this dual nature; however, concentration and physiochemical state (bound by calcium, oxidation state, dimerization) of the protein appear to be involved. The form of S100B with mitogenic activity is in an oxidized state (Kligman & Marshak, 1985; Selinfreund et al., 1991; Barger et al., 1992; Scotto et al., 1998) and the neurotrophic activities depend on a disulfide-linked dimeric form of the protein and the presence of two cysteine residues capable of irreversible redox-based modifications (Scotto et al, 1998; Koppal et al., 2001; Zhukova et al., 2004). Typically, S100B accumulates in glial cells in the reduced form that has no activity in inducing neurite extension (Scotto et al., 1998). However, the structural features of S100B that promote neurotrophic activity are different than

those affecting glial activation activity. Those proteins lacking one or both of the cysteine residues are capable of inducing pro-inflammatory neurotoxic responses from microglia cells through the production of IL-1β and inducible nitric oxide synthase (iNOS).

It is not yet known how either the reduced or oxidized form of extracellular S100B exerts its effects on target cells. The protein may either effect cells directly when internalized or through cell surface receptors such as RAGE (receptor for advanced glycation endproducts) on neurons or glia (Huttunen et al., 2000; Donato, 2007). Many, but not all, of the cellular actions of S100B are mediated through activation of RAGE where increased levels of S100B can lead to its upregulation. Thus, S100B/RAGE interactions can lead to the neuroinflammatory processes and pathological changes in neurons and glial cells.

RAGE

Increased levels of S100B are also thought to lead to increases in RAGE and this receptor is involved in many, but not all, of the actions of S100B. RAGE is a known cell surface multiligand receptor for S100B that responds to a number of ligands of different structures including AGE's (advanced glycation endproducts), amyloid fibrils, amphoterins and S100/calgranulin family of proteins. In the central nervous system, RAGE can be localized to neurons, microglial cells and astrocytes. The RAGE receptor is a member of the immunoglobulin superfamily and leads to cellular dysfunction in a number of disorders. It was originally identified and characterized for its binding of advanced

gylcation endproducts (AGEs), which are formed by glycoxidation. These AGE's accumulate in disorders such as diabetes and renal failure (Neeper et al., 1992). Other pathological processes involving these ligands and the RAGE receptor include AD, Parkinson's disease (PD), Creutzfeldt-Jakob disease and Huntington's chorea.

RAGE expression has an unusual sustained juxtaposition of ligand and receptor and is thought to be upregulated by the presence of its own ligands. There are relatively low levels of RAGE expression found in typical tissue, but when high levels of its ligands such as S100B are found, RAGE expression increases as well (Schmidt et al., 2000). Binding of ligands to this receptor leads to activation of signaling pathways which in turn can modulate gene expression (Matsunaga et al., 2002). One such pathway activated is that of the proinflammatory transcription factor NFκB which leads to subsequent expression of NFκB- regulated cytokines (Haslbeck et al., 2004). NFκB typically exists in a latent cytoplasmic form until stimulation by receptor ligands such as S100B upon the RAGE receptor. Upon stimulation, NFκB activates rapidly and translocates to the nucleus by a release of an inhibitory binding protein IκB via its phosphorylation (Domanska-Janik et al., 2001). These proinflammatory cytokines that are then released include interleukin (IL)-1β, IL-6 and tumor necrosis factor-α. Pro-inflammatory cytokines refer to non-antibody proteins that act as intercellular mediators and are capable of producing cellular and neuronal damage.

Microglia

Because S100B is suspected to be found on microglia in the central nervous system, it is expected that RAGE will be localized as well. The innate immune system of the central nervous system is composed of microglial cells that are involved in antigen presentation and immune-response generation of cytokines (Streit, Mrak, & Griffin, 2004). When trauma or disease damages the brain, microglia expressing the RAGE receptor react (Leong & Ling, 1992). These cells migrate to the site of injury (Mitchell et al., 1993) and proliferate. Microglial cells are found in various morphological states that correlate with distinct functional states of resting, reactive and chronically active (Streit et al., 1988). Microglia are typically found in the resting state in which they bear thin ramified processes that emerge from the cell body to perform basic monitoring and homeostatic activities. Under certain conditions such as with general increases in age, neurodegenerative diseases like AD or with acute injury, microglia become reactive, retract their processes and increase the expression of different molecules. These molecules include cytokines, growth factors and free radicals while the microglia become macrophages of the CNS that can phagocytose neurons that have been damaged or are dying (Streit et al., 1999). Available evidence suggests in rodents, non-human primates and humans that there is apparent microglial activation associated with aging (Streit, Sammons, Kuhns, & Sparks, 2004) with chronic activation and neuroinflammation processes being found in AD.

In a case of acute neuroinflammation, activation is considered to be beneficial to restoring the homeostasis of the brain when activated cells are neuroprotective by removing debris after injury. They are also effective at clearance of the β-amyloid (Aβ) protein involved in plaque and neurofibrillary tangle formation of AD (Frackowiak et al., 1992). However, the ability of adult microglial cells to degrade proteins is substantially decreased in comparison to cells from newborn animals (Stolzing et al., 2006). In the aged brain, the neuroprotective role of these cells may be decreased as suggested by the presence of dystrophic microglia cells with structural deterioration (Streit, Sammons, Kuhns, and Sparks, 2004) and apoptotic markers (Lassmann et al., 1995; Drache et al., 1997).

It is thought that chronic intermittent neuroinflammation and activation of microglial cells is damaging to the brain and may lead directly to the neurodegeneration as opposed to neuroprotection. A constant attempt and inability of amyloid phagocytosis may lead activated cells to over-produce neurotoxic inflammatory products such as cytokines and reactive oxygen species (Griffin et al., 1989; Griffin et al., 1998b; Akiyama et al., 2000; McGeer & McGeer, 2001; Rogers et al., 2002; Streit, 2004; Block et al., 2007). Chronic activation may not only lead directly to neurodegenerative changes, but eventually to microglial cell senescence and further impaired neuroprotection (Streit, 2004). S100B/RAGE interactions on microglial activation are thought to be involved in these neuroinflammatory processes. Although the direct

mechanism is not known, chronic activation may be enhanced through the heightened levels of S100B on the RAGE receptor located on microglial cells.

Chronic neuroinflammation may increase the amount of cognitive damage in AD when the activated glia and resulting pro-inflammatory cytokines are concentrated in the learning and memory center of the hippocampus (Cagnin et al., 2001). Within the hippocampus, activated microglial cells are associated with increases in neurofibrillary tangle formations. (Dipatre & Gelmann, 1997). The progression of damage in AD follows a highly predictable pattern, first spreading from the entorhinal cortex to the subiculum to where it then affects the CA1 hippocampal subfield followed by the CA2, CA3 and eventually CA4 regions and dentate gyrus (Schonheit et al., 2004).

S100B/RAGE interactions are thought to be involved in these neuroinflammatory processes involving microglial activation. Therefore, it is possible that over-expression of S100B would lead to increases in binding to the RAGE receptor located on neurons as well as microglia. This continued increase of binding to the RAGE receptor may possibly lead to an increase in NFκB activation with elevated cytokine production via microglial activation leading to a chronic neuroinflammatory state and neuronal damage as is possible in AD.

Vitamin E

Although previous research has provided mixed results, it has been suggested that antioxidants such as Vitamin E (dl-alpha tocopheryl acetate) can prevent neuronal damage induced by neuroinflammation (Wang et al., 2006) and may be an effective treatment in neuroinflammatory illnesses such as AD (Liu et

al., 2007), (PD) (Singh et al., 2007) and DS (Perrone et al., 2007) by reducing the extent of oxidation (Pratico, 2001).

A recent paper suggested nutritional factors including Vitamin E begun prenatally may help prevent mental deterioration due to oxidative stress (Liu et al., 2007; Thiel & Fowkes, 2005). In animals, prolonged dietary Vitamin E intake was shown to slow the onset of oxidative damage and attenuate the loss of cognitive and motor performance (Joseph et al., 1998). In the Tg2576 mouse model of AD, Vitamin E supplementation in the young, but not old, reduced Aβ levels and amyloid deposition (Sung et al., 2003) and delayed the development of tau pathologies in mice over-expressing the human tau protein (Nakashima et al., 2004).

The potentially therapeutic use of Vitamin E in clinical trials (Sano et al., 1997; Grundman et al., 2002) and the positive evidence from animal models of AD supported the rationale to provide early Vitamin E supplementation to the S100B over-expressing mouse model of neuroinflammatory-induced pathological aging. The S100B transgenic mice have previously displayed accelerated age-related deficits including loss of dendritic and synaptic markers (Shapiro & Whitaker-Azmitia, 2004), increased expression of apoptotic markers (Shapiro et al., 2004) and losses in learning and memory (Gerlai et al., 1994; Gerlai & Roder, 1995; Gerlai, & Roder, 1996; Winocur et al., 2001; Bell et al., 2003). S100B itself may be largely in an oxidized state in the neuropil and thus treatment with an antioxidant such as Vitamin E may have effects on the protein and it's interaction with RAGE and microglia.

Experiment 1: S100B, RAGE and microglial activation

The first experiment is designed to determine the influence of increased S100B expression throughout development and aging on the transitional states of microglia and the RAGE receptor using an S100B over-expressing mouse model of DS and pathological aging. Because S100B is triplicated in DS at the earliest stages of development and most individuals with the disorder go on to develop Alzheimer's disease at an early age, the S100B-overexpressing mouse provides a model to study both the beginning stages of pathological development as well as the effects of accelerated aging within one organism. The S100B transgenic mice used in the current study have previously been shown to display accelerated age-related neuronal damage, including loss of dendritic and synaptic markers (Shapiro & Whitaker-Azmitia, 2004) and an increased expression of apoptotic markers (Shapiro et al., 2004) as well as losses in learning and memory (Gerlai et al., 1994; Gerlai & Roder, 1995; Gerlai & Roder, 1996; Winocur et al., 2001; Bell, et al., 2003). Tissue levels of S100B continue to remain elevated throughout the life of the transgenic animal and astroglial cells are releasing high amounts of S100B into the neuropil (Shapiro, 2003).

The morphological transitions of microglia, RAGE immunoreactivity, and neuronal counts will be determined throughout the lifespan of the animal as compared to controls as described in detail below. Although many studies have suggested that increased microglial activation, RAGE upregulation and neuronal damage are associated with aging, particularly in AD and DS, no studies have provided a framework in which to quantify these throughout the lifespan from

development to aging. Lifespan quantification of these cellular mechanisms will provide further support of the S100B over-expressing mouse as a model of both DS and AD in the context of neuroinflammation for future studies.

Experiment 2: Vitamin E Supplementation

The second experiment will focus on the role of antioxidants, particularly Vitamin E, in the potential attenuation of neuroinflammatory damage associated with increased S100B and microglial activation. S100B itself may be largely in an oxidized state in the neuropil and thus treatment with an antioxidant such as Vitamin E may have effects on the protein and it's interaction with RAGE and microglia. Although the direct molecular mechanism is not known, it will be assessed whether Vitamin E has the potential to induce or inhibit a transition of microglial cells from a resting to an activated state in the S100B over-expressing mice and CD1 control mice during development and aging.

Because S100B is increased in both the neurodengenerative disorder of AD and in the developmental pathology of DS, it provides a potential target of therapeutic intervention at both an early developmental stage and at a later stage of pathological aging. An early and late intervention diet supplemented with Vitamin E may protect the brain of animals with high developmental levels of S100B against oxidative stress or possibly mediate the damage caused by neuroinflammatory processes occurring during aging. S100B itself may be largely in an oxidized state in the neuropil and thus treatment with an antioxidant such as Vitamin E may have direct effects on the protein and it's interaction with RAGE and microglia. The potentially therapeutic use of Vitamin E in clinical trials

(Sano et al., 1997; Grundman et al., 2002) and the positive evidence from animal models of AD support the rationale to provide Vitamin E supplementation to the S100B over-expressing mouse model of neuroinflammatory-induced pathological aging. None of these previous studies have determined whether the supplementation of Vitamin E can attenuate the activation of microglial or neuronal loss when given during development as a preventative to damage (Experiment 2a) or given as a treatment during aging (Experiment 2b).

Method Experiment 1

Animals

The S100B mice (as described previously in Friend et al., 1992; Gerlai et al., 1994; Shapiro et al., 2004; Shapiro & Whitaker-Azmitia, 2004) and their congenic CD1 controls used in this experiment were bred and raised in the animal care facilities at SUNY Stony Brook in identical conditions of a 12-h light and 12-h dark cycle. Animals are provided free access to standard lab chow (Prolab® RMH 3000) and water.

Tissue preparation

At 30, 90, 180, and 365 days of age (n=6 per age per strain (CD1 or S100B) for at total of 48), animals were anesthetized with a 10 mg/kg xylazine/ketaset mixture (7:5) and transcardially perfused with .9% normal saline (approximately 50ml or until effluent ran clear) followed by 4% paraformaldehyde lysine prill (PLP) in phosphate buffer (7.2 pH; approximately 50ml or until neck, limbs and tail were rigid). The brains were removed and postfixed for 24-h in 4% PLP then

cryo-protected in a series of sucrose (10%, 20% and 30%) for 24-h each. Brain tissue was sectioned at 40 µm on a sliding microtome with a freezing stage (American Optical Corporation) and collected into phosphate-buffered saline (PBS; pH 7.2; 0.01M) containing .1% sodium azide. Six-well plates were used for tissue collection allowing each brain to be stained with a maximum of 6 antibodies with a minimum of 210 µm between each slice to eliminate the possible double counting of cells. Following collection, tissue sections will be transferred to eight-chamber Plexiglas staining trays with mesh bottoms that fit into a petri dish containing antibodies or washing buffer. This allowed for identical staining of animals counterbalanced throughout the baskets.

Immunohistochemistry

Microglia

Total microglia, both resting and activated, will be visualized using the monoclonal rat anti-mouse F4/80 primary antibody (1:1000; Serotec # MCA497R). F4/80 was chosen for the identification of microglia because it has been shown to be a monoclonal antibody directed specifically against the murine macrophage including microglia in the developing and adult mouse brain as previously described by Austyn and Gordon, 1981 and Perry et al., 1985. Sections were incubated in primary antibody on a cold rotator for 36-h at 4º C until the tissue is rinsed in three PBS (7.2 pH) baths for 5 min each bath followed by incubation with a biotinylated secondary Anti-Rat IgG antibody (1:200, Vector BA-9400) for 1.5-h at room temperature. The tissue is again rinsed for 3 times 5 mins each bath in PBS (7.2 pH for 5 min in each bath) then transferred to an

avidin-biotin complex (ABC; 1:100; Vector Labs ABC Elite Kit # PK2200) for 1-h rotating at room temperature. Following the ABC reaction, microglial immunoreactivity was visualized using .05% 3,3'diaminobenzadine (DAB) in Trizma buffer (pH 7.2; Sigma; T0194) for 3 min followed by the addition of 35µl of 30% hydrogen peroxide/100ml of DAB solution for 3-min. After 3-min, the reaction is halted in 0.01 M PBS (pH 7.2) and then rinsed in 3 baths of PBS for 5-min each. Serial brain sections are then mounted on gelatin-coated slides, dehydrated with an ethanol series (70%, 90%, 100%), cleared in three 2-min xylene baths and cover slipped.

RAGE

RAGE immunoreactivity was visualized by incubation in a rabbit polyclonal anti-RAGE primary antibody (1:250; Affinity BioReagents PA1-075) for 36-h on a cold rotator at 4℃ followed by incubation with biotinylated secondary antibody (1:200; Sigma anti-Rabbit IgG # B7389) for 1.5- h at room temperature. ABC, DAB and mounting procedures are similar to those described above for microglial reactivity.

Neuronal density was determined using the nissl stain of cresyl violet. The nissl substance, the rough endoplasmic reticulum of neurons, appears dark blue to violet due to the staining of the ribosomal RNA. This provides staining of the cell body cytoplasm as well as the DNA of the nucleus of neurons. Nissl substance is known to be lost after cell injury and density of staining will provide a means of quantifying neuronal degeneration.

Double-labeling RAGE and Microglia

To verify the presence of the RAGE receptor on microglial cells, double labeling immunocytochemistry was conducted using RAGE (Affinity BioReagents PA1-075) and F4/80 (Serotec # MCA497R) primary antibodies. F4/80 immunocytochemistry visualized with DAB was conducted as previously described. Tissue was rinsed and incubated 36-h rotating at 4℃ in rabbit polyclonal anti-RAGE primary antibody (1:200; Affinity BioReagents PA1-075) then incubated with a biotinylated secondary antibody (1:200; Sigma anti-Rabbit IgG) for 1.5-h at room temperature. Tissue was rinsed, transferred to ABC (1:100; Vector Labs ABC Elite Kit # PK2200) for 1-h rotation at room temperature, rinsed again, then visualized using Vector Blue Alkaline Phosphatase Substrate Kit III (Vector Labs; Sk-5300) by development in Vector Blue substrate working solution as prepared by manufacturer's instructions for 30 mins rotating at room temperature in the dark. Tissue was rinsed in 100mM Tris-HCL (pH 8.2) buffer, mounted, dehydrated through a series of ethanol, cleared (Histoclear), and cover-slipped using crystalline.

Standardized Optical Density Measurements

Slides were coded to ensure unbiased image capture and analysis. Images were taken using an Olympus BH-2 light microscope with a mounted digital Tripix camera (Electroimage Tripix TM, Tetracam, Great Neck, NY). Using a light intensity meter lock, light intensity was maintained at a constant level for all images saved on a Windows based PC that used the University of Texas Image Tool Software (UTHSCSA, Version 3.0). Using UTHSCSA, images were

calibrated to a known optical density gray scale value using the Kodak step tablet # 2 as described by Shapiro and Whitaker-Azmitia (2004). The grayscale calibration images were captured at the same light intensity and microscope settings as the brain sections.

For this study, the regions of interest examined included the hippocampal subfields of CA1 and CA3 including the pyramidal cells, stratum oriens, stratum radiatum as well as the hilus, upper blade and lower blade of the dentate gyrus. The hippocampus is selected for analysis based on previous data suggesting it's vulnerability within the S100B over-expressing mouse as well as it's degeneration associated with Alzheimer's disease and early memory deficits. Fig. 1 is a schematic representation of how the regions are to be delineated for measurement based on stereotaxic mouse coordinates of Paxinos & Franklin (2001) and corresponded to -1.46 and -2.30 mm from bregma. Within each designated region of interest, three sample areas of 1,500 μm^2 spaced 150 μm apart per 40 μm slice are taken. This provides approximately 12 sample areas of each region of interest (CA 1 pyramidal for example) to be averaged for each region of interest per animal.

Statistical Analysis

A 2 x 4 repeated measures analysis of variances (ANOVA) was performed on the data for S100B and CD1 control mice at all four ages (30, 90, 180, and 365 days) for the dependent variables of microglia and RAGE immunoreactivity and cresyl violet optical density. This provides for the analysis of the main effects and interactions of the two independent variables: strain (between-

subjects; S100B or control) and age (within-subjects; 30, 90, 180, and 365 days) for each mentioned dependent variable. Significant between-subjects results will indicate that higher levels of S100B (main effect of strain) result in differences in immunoreactivity for RAGE, microglia and/or cresyl violet neuronal density. Significant within-subject results will indicate that differences in immunoreactivity for RAGE, microglia and/or cresyl violet neuronal density are age dependent (levels vary from development to aging). This led to multiple pair-wise comparisons using simple independent t-tests, ANOVAs and post-hoc Bonferroni tests that determined where specific age effects were found for each strain. In summary, these statistics will determine if 1: higher levels of S100B have an effect on the amount of RAGE, microglia, and neuronal density and 2: this immunoreactivity changes with the age of the animal.

Method Experiment 2

Animals and Tissue Preparation

Dietary supplement

Experiment 2a: Pregnant dams of each strain (control or S100B over-expressing) were divided into 4 dietary groups of either control chow or Vitamin E supplemented diet. The control chow used was Prolab® RMH 3000 while the experimental Vitamin E supplemented diet was produced by Purina® Test Diet by mixing 975 IU/kg of dl-alpha tocopheryl acetate (Vitamin E) uniformly into the Prolab® RMH 3000 for a total of 1,000IU/kg of food. Pregnant dams were given their respective diet during three days prior to conception as well as throughout

pregnancy and nursing. At weaning (PND 21), male pups from different litters were assigned to one of four groups (CD1 control chow (CC) n = 4; S100B control chow (SC) n = 4; CD1 Vitamin E supplemented diet (CE) n = 4; S100B Vitamin E supplement diet (SE) n =4) and were provided water and food *ad libitum* consistent with their dietary designation for a total of 16 animals in the study. Animals ate on average 50 IU/kg of body weight daily. Animals were sacrificed at PND 165 (5.5 months). This age was selected for two reasons: 1- animals were becoming significantly overweight on the diet and health of the animals became a concern; 2- this age would allow for the assessment of tissue immunoreactivity as a result of the diet on development as opposed to the counteracting affects of aging.

Experiment 2b: A separate series of animals (n=16) were divided into the same groups as described as above. In contrast to the above experiment, animals were provided control chow from weaning until 150 days of age (5 months) and then designated animals were then given the Vitamin E supplemented diet until approximately 300 days of age (10 months). These ages were chosen to assess the effects of dietary supplementation on aging as opposed to development of the organism.

Immunohistochemistry and Analysis

Animals in both Experiment 2a and 2b were sacrificed at their designated ages and immunocytochemistry for microglia, RAGE and neuronal density (Experiment 2b only) were performed as described above (see Experiment 1). For Experiment 2a, relative optical density measurements were taken whereas

standardized optical density measurements using the Kodak Step Tablet were done for Experiment 2b (as described in Experiment 1). In Experiment 2a, activated microglial cells were individually counted as microglial cells have a cell body of 16 μm or greater and less than three ramified processes as well as included in total optical density measurements. Individual counts were not possible for Experiment 2b due to densely populated regions of activated cells and therefore optical density measures were only performed. Data were analyzed using multivariate analysis of variance designs using a two-way (ANOVA) in each experiment. The 2 (S100B or control) x 2 (control or Vitamin E diet) design determined main effects of both the strain of the animal and it's diet as well as a potential interaction of the two on immunoreactivity. *Post hoc* Bonferroni analysis will determine where, if any, significant differences were found.

Results: Experiment 1

Co-localization of RAGE and microglia

Double labeling immunocytochemistry revealed co-localization of RAGE positive cells and total microglia (resting and activated morphology as depicted in Fig. 2) in the hippocampus of the S100B over-expressing transgenic mouse on a control diet as shown in Fig. 3. Although resting and activated microglia cells can be seen, RAGE appears to have the highest pattern of co-labeling with activated cells in the pyramidal region as opposed to the majority of cells in the resting form in the dendritic regions of stratum oriens and radiatum. This is significant in

that resting microglia cells remain in the dendritic regions whereas activated cells bearing the RAGE receptor are in regions containing neuronal cell bodies.

Microglia Immunodensity at 1, 3, 6 and 12 months of age

A 2 (Strain: CD1 or S100B) X 4 (Age: 1, 3, 6 or 12 months) repeated measures ANOVA revealed significant main effects of strain and age as well as a significant interaction of age x strain as shown in Table 1 for regions of interest including CA1 stratum oriens, CA1 pyramidal, CA1 stratum radiatum, CA3 stratum oriens, CA3 pyramidal upper blade of the dentate gyrus and lower blade of the dentate gyrus. CA3 stratum radiatum and hilus of the dentate gyrus displayed only a significant main effect of age. Main effect of strain and the interaction of age x strain were not significant in these regions of interest. Mean standardized optical density measurements for total microglia in both the resting and activated form for CD1 and S100B-overexpressing mice are shown in Table 2 for each age of the CD1 control and S100B-overexpressing as depicted in Fig. 4 and Fig. 5 respectively.

Table 1

Microglia Immunoreactivity 2 X 4 Repeated Measures ANOVA for CD1 and S100B-overexpressing Animals at 1, 3, 6 and 12 Months of Age

Region of Interest	Effect/Interaction	Statistical Significance
CA1 stratum oriens	Strain	F (1, 10) = 212.57, $p = 0.00$*
	Age	F (3, 30) = 428.43, $p = 0.00$*
	Age x Strain	F (3, 30) = 43.14, $p = 0.00$*
CA1 pyramidal	Strain	F (1, 10) = 19014.88, p = 0.00*
	Age	F (3, 30) = 3021.20, p = 0.00*
	Age x Strain	F (3, 30) = 1645.68, p = 0.00*
CA1 stratum radiatum	Strain	F (1, 10) = 14.66, p = 0.003*
	Age	F (3, 30) = 497.30, p = 0.00*
	Age x Strain	F (3, 30) = 10.57, p = 0.00*
CA3 stratum oriens	Strain	F (1, 10) = 125.92, p = 0.00*
	Age	F (3, 30) = 455.40, p = 0.00*
	Age x Strain	F (3, 30) = 11.97, p = 0.00*
CA3 pyramidal	Strain	F (1, 10) = 52.58, p = 0.00*
	Age	F (3, 30) = 54.21, p = 0.00*
	Age x Strain	F (3, 30) = 16.48, p = 0.00*
CA3 stratum radiatum	Strain	F (1, 10) = 1.75, p = 0.215
	Age	F (3, 30) = 19.97, p = 0.00*
	Age x Strain	F (3, 30) = 1.69, p = 0.191
Upper blade dentate gyrus	Strain	F (1, 10) = 550.93, p = 0.00*
	Age	F (3, 30) = 2128.28, p = 0.00*
	Age x Strain	F (3, 30) = 772.12. p = 0.00*
Lower blade dentate gyrus	Strain	F (1, 10) = 265.30, p = 0.00*
	Age	F (3, 30) = 711.54, p = 0.00*
	Age x Strain	F (3, 30) = 335.37, p = 0.00*
Hilus dentate gyrus	Strain	F (1, 10) = 2.00, p = 0.191
	Age	F (3, 30) = 19.24, p = 0.00*
	Age x Strain	F (3, 30) = 1.88, p = .0.154

Note. * significance at $p < .005$; Sphericity Assumed

Table 2

Mean Standardized Optical Density Measurements for Total Microglia in both the Resting and Activated form for CD1 and S100B-overexpressing Mice

Region of interest	Age (months)	Optical Density	Standard Deviation
CA1 stratum oriens			
CD1	1	0.0178	0.0046
	3	0.1605	0.0372
	6	0.2182	0.0195
	12	0.2173	0.0185
S100B	1	0.0182	0.0046
	3	0.1968	0.0046
	6	0.3367	0.0388
	12	0.4031	0.0041
CA1 pyramidal			
CD1	1	0.0035	0.0029
	3	0.0145	0.0020
	6	0.0143	0.0028
	12	0.0350	0.0032
S100B	1	0.0065	0.0032
	3	0.0301	0.0005
	6	0.0566	0.0035
	12	0.1962	0.0037
CA1 stratum radiatum			
CD1	1	0.0117	0.0040
	3	0.1005	0.0003
	6	0.1909	0.0011
	12	0.2222	0.0357
S100B	1	0.0133	0.0037
	3	0.1006	0.0007
	6	0.1897	0.0212
	12	0.2837	0.0153
CA3 stratum oriens			
CD1	1	0.0129	0.0005
	3	0.1294	0.0544
	6	0.2205	0.0204
	12	0.2962	0.0038
S100B	1	0.0168	0.0005
	3	0.1972	0.0037
	6	0.3212	0.0276
	12	0.4022	0.0084
CA3 pyramidal			
CD1	1	0.0020	0.0008
	3	0.0182	0.0028
	6	0.0158	0.0002
	12	0.0431	0.0212

Table 2 con't

Region of interest	Age (months)	Optical Density	Standard Deviation
CA3 pyramidal			
S100B	1	0.0020	0.0006
	3	0.0252	0.0030
	6	0.0520	0.0039
	12	0.1317	0.0423
CA3 stratum radiatum			
CD1	1	0.0136	0.0031
	3	0.1042	0.0047
	6	0.1961	0.0040
	12	0.2485	0.0421
S100B	1	0.0185	0.0024
	3	0.1056	0.0076
	6	0.1930	0.0092
	12	0.4032	0.2871
Upper blade dentate gyrus			
CD1	1	0.0014	0.0004
	3	0.0138	0.0024
	6	0.0171	0.0022
	12	0.0308	0.0041
S100B	1	0.0014	0.0005
	3	0.0132	0.0020
	6	0.0233	0.0029
	12	0.0993	0.0008
Lower blade dentate gyrus			
CD1	1	0.0013	0.0000
	3	0.0127	0.0008
	6	0.0164	0.0017
	12	0.0242	0.0030
S100B	1	0.0021	0.0019
	3	0.0132	0.0034
	6	0.0239	0.0788
	12	0.0978	0.0041
Hilus			
CD1	1	0.0137	0.0031
	3	0.1043	0.0047
	6	0.1957	0.0046
	12	0.2382	0.0350
S100B	1	0.0189	0.0024
	3	0.1055	0.0077
	6	0.1930	0.0092
	12	0.4017	0.2878

Note. Mean Standardized Optical Density if an average of n=6 per strain at each age for a total of N = 48 animals.

Microglia post hoc analysis CA1 - Fig 6.

Independent *post hoc t*- test analysis of CA1 stratum oriens revealed a significant difference between CD1 and S100B-overexpressing mice at 3 months, t (10) = -2.378, p <0.05; 6 months, t (10) - 6.691, p = 0.00; and 12 months of age, t (10) = -24.052, p = 0.00 with S100B-overexpressing mice having significantly greater microglial immunoreactivity than controls. Within-subject ANOVA analysis of CD1 mice suggested significant reactivity increases with age, F (3, 20) = 100.47, p = 0.00, specifically 1 month animals had significantly less reactivity than 3, 6, and 12 month old animals, p = 0.00 and 3 month old animals had significantly less reactivity than 6 or 12 month animals, p < 0.005. No significant differences were found between 6 and 12 month CD1 control animals, p > 0.05. Within subject analysis of S100B-overexpressing animals revealed significant increases in immunoreactivity with age, F (3, 20) = 438.42, p = 0.00, will all ages significantly different from each other, p = 0.00.

Independent *post hoc t*-test analysis of CA1 pyramidal region similarly revealed that S100B mice has significantly greater microglial immunoreactivity at 3 months, t (10) = -18.33, p =0.00; 6 months, t (10) = 23.088, p = 0.00; and 12 months of age, t (10) -= -79.904, p = 0.00 compared to CD1 control animals. Within subjects comparisons of CD1 control animals showed significant difference between ages, F (3, 20) = 137.007, p = 0.00. Specifically 1 month animals had significantly less reactivity than all other ages, p = 0.00 and 12 month animals had significantly greater immunoreactivity than all other age groups, p = 0.00. Within subject analysis of S100B-overexpressing animals

revealed significant increases in immunoreactivity with age, F (3, 20) = 4733.935, $p = 0.00$, will all ages significantly different from each other, $p = 0.00$.

Independent *post hoc t*-test analysis of CA1 stratum radiatum showed that S100B mice had significantly greater immunoreactivity than control animals only at 12 months of age, $t\,(10) = -3.872$, $p < 0.01$. Within subject analysis of CD1 control, F (3, 20) = 167.894, $p = 0.00$, and S100B mice, F (3, 20) = 463.824, $p = 0.00$, show increases in reactivity between all ages, $p < 0.05$.

Microglia post hoc analysis CA3 - Fig. 7

Independent *post hoc t*- test analysis of CA3 stratum oriens revealed a significant increase in microglial immunoreactivity of S100B-overexpressing mice as compared to CD1 control animals at all ages of 1 month $t\,(10) = -3.194$, $p = 0.01$; 3 month $t\,(10) = -3.050$, $p < 0.02$; 6 month $t\,(10) = -7.186$, $p = 0.00$; and 12 months of age $t\,(10) = -28.161$, $p = 0.00$. Within subject analysis of CD1 control, F (3, 20) = 105.646, $p = 0.00$, and S100B mice, F (3, 20) = 791.528, $p = 0.00$, show increases in reactivity between all ages, $p < 0.001$.

Independent *post hoc t*- test analysis of CA3 pyramidal revealed a significant increase in microglial immunoreactivity in S100B-overexpressing mice as compared to controls at 3 month $t\,(10) = -4.123$, $p < 0.005$, 6 month $t\,(10) = -22.820$, $p = 0.00$, and 12 months of age $t\,(10) = -4.591$, $p = 0.001$. Within subjects comparisons showed that CD1 control animals, F (3, 20) = 15.354, $p = 0.00$, and S100B mice, F (3, 20) = 42.261, $p = 0.00$, had significantly greater reactivity with age in that 12 month animals had more microglia than all other age groups, $p < 0.005$.

Within subject age comparisons in CA3 stratum radiatum of CD1 control animals revealed a significant increase in immunoreactivity with age, F (3, 20) = 141.28, $p = 0.00$, with all ages significantly different from each other, $p < 0.005$. Within subject age comparisons of S100B mice showed significant increases in immunoreactivity with age, F (3, 20) = 7.904, $p = 0.001$ with 12 month animals having significantly greater immunoreactivity than 1 or 3 month old animals, $p < 0.05$.

Microglia post hoc analysis dentate gyrus - Fig. 8

Independent *post hoc t*- test analysis of the upper blade of the dentate gyrus revealed a significant increase in microglial immunoreactivity of S100B-overexpressing mice as compared to CD1 control animals at 6 months, t (10) = -4.156, $p < 0.005$ and 12 months of age, t (10) = -40.341, $p = 0.00$. Within subject age comparisons of CD1 control animals revealed increases in microglial density, F (3, 20) = 125.377, $p = 0.00$ with 1 month animals having significantly less density and 12 month animals having significantly greater density than all other age groups, $p = 0.00$. Within subjects comparison of S100B mice revealed significant differences between all age groups, $p = 0.00$.

Independent *post hoc t*- test analysis of the lower blade of the dentate gyrus revealed a significant increase in microglial immunoreactivity of S100B-overexpressing mice as compared to CD1 control animals at 6 months t (10) = -2.292, $p < 0.05$ and *12* months of age, t (10) = -35.56, $p = 0.00$. Within subject age comparisons of CD1 control F (3, 20) = 172.02, $p = 0.00$ and S100B mice F

(3, 20) = 481.646, $p = 0.00$ revealed significant increases in microglial density with increasing age between all age groups, $p < .05$.

Within subject age comparisons of the hilus of CD1 control animals revealed a significant increase in immunoreactivity with age, F (3, 20) = 188.094, $p = 0.00$, with all ages significantly different from each other, $p < 0.005$. Within subject age comparisons of the hilus of S100B mice revealed significantly difference in age associated reactivity, F (3, 20) = 7.790, $p = 0.001$, with 12 month animals have greater reactivity than 1 and 3 month old animals, $p < 0.05$.

RAGE Immunodensity at 1, 3, 6 and 12 months of age

A 2 (Strain: CD1 or S100B) X 4 (Age: 1, 3, 6 or 12 months) repeated measures ANOVA revealed significant main effects of strain and age as well as a significant interaction of age x strain as shown in Table 3 for hippocampus regions of interest as depicted in Fig. 9, including CA1 pyramidal, CA3 pyramidal and the upper blade of the dentate gyrus for RAGE immunoreactivity. No significant differences were found in the lower blade and hilus of the dentate gyrus. Average RAGE standardized optical density measurements for CD1 and S100B-overexpressing mice are shown in Table 4 for each age.

Table 3

RAGE Immunoreactivity 2 X 4 Repeated Measures ANOVA for CD1 and S100B-overexpressing Animals at 1, 3, 6 and 12 Months of Age

Region of Interest	Effect/Interaction	Statistical Significance
CA1 pyramidal	Strain	F (1, 10) = 6.055, $p < 0.05$*
	Age	F (3, 30) = 11.849, p=0.00*
	Age x Strain	F (3, 30) = 7.414, p=0.001*
CA3 pyramidal	Strain	F (1, 10) = 5.842, $p < 0.05$*
	Age	F (3, 30) = 7.402, p=0.001*
	Age x Strain	F (3, 30) = 7.645, p= 0.001*
Upper blade	Strain	F (1, 10) = 5.622, $p < 0.05$*
Dentate gyrus	Age	F (3, 30) = 5.334, p=0.005*
	Age x Strain	F (3, 30) = 3.151, $p < 0.05$*
Lower Blade	Strain	F (1, 10) = 3.940, $p > 0.05$
Dentate Gyrus	Age	F (3, 30) = 1.401, $p > 0.05$
	Age x Strain	F (3, 30) = 1.787, $p > 0.05$
Hilus	Strain	F (1, 10) = 3.815, $p > 0.05$
Dentate Gyrus	Age	F (3, 30) = 0.585, $p > 0.05$
	Age x Strain	F (3, 30) = 0.673, $p > 0.05$

Note. * significance at $p < .005$; Sphericity Assumed

Table 4

Mean RAGE Standardized Optical Density Measurements for CD1 and S100B-overexpressing Mice

Region of interest	Age (months)	Optical Density	Standard Deviation
CA1 Pyramidal			
CD1	1	0.0528	0.0523
	3	0.0631	0.0580
	6	0.0837	0.0818
	12	0.0911	0.0865
S100B	1	0.1093	0.0267
	3	0.1504	0.0320
	6	0.1402	0.0808
	12	0.1148	0.0330
CA3 pyramidal			
CD1	1	0.0575	0.0549
	3	0.0686	0.0622
	6	0.0832	0.0808
	12	0.1033	0.0567
S100B	1	0.1225	0.0436
	3	0.1486	0.0288
	6	0.1981	0.0124
	12	0.1154	0.0326
Upper blade dentate gyrus			
CD1	1	0.0574	0.0519
	3	0.0686	0.0625
	6	0.0836	0.0796
	12	0.0999	0.0783
S100B	1	0.1256	0.0548
	3	0.1352	0.0222
	6	0.1880	0.0099
	12	0.1321	0.07829
Lower blade dentate gyrus			
CD1	1	0.0574	0.0519
	3	0.0686	0.0625
	6	0.0746	0.0717
	12	0.0999	0.0783
S100B	1	0.1256	0.0548
	3	0.1352	0.0222
	6	0.1284	0.0188
	12	0.1321	0.0454

Table 4 con't

Mean RAGE Standardized Optical Density Measurements for CD1 and S100B-overexpressing Mice

Region of interest	Age (months)	Optical Density	Standard Deviation
Hilus dentate gyrus			
CD1	1	-0.1021	0.0309
	3	-0.1036	0.0304
	6	-0.1019	0.0304
	12	-0.0973	0.0346
S100B	1	-0.0294	0.0938
	3	-0.0594	0.0748
	6	-0.0113	0.1264
	12	-0.0599	0.0591

Note. Mean Standardized Optical Density if an average of n=6 per strain at each age for a total of N = 48 animals.

RAGE post hoc analysis CA1 pyramidal

Independent *post hoc t*- test analysis of CA1 pyramidal revealed a significant difference between CD1 and S100B-overexpressing mice at 1 month, t (10) = -2.355, p <0.05; 3 months, t (10) - 3.227, p < 0.01; and 6 months of age, t (10) = -3.38, p < 0.01 with S100B-overexpressing mice having significantly greater RAGE immunoreactivity than controls as shown in Fig 10. Within-subject ANOVA analysis of S100B mice suggested significant reactivity difference with age, F (3, 20) = 13.699, p = 0.00, specifically 6 month old animals had significantly greater reactivity than 1 and 3 month old animals but less than 12 month old animals, p < 0.05. No significant age differences were found within CD1 control animals, F (3, 20) = 0.375, p > 0.05.

RAGE post hoc analysis CA3 pyramidal

Independent *post hoc t*- test analysis of CA3 pyramidal revealed a significant difference between CD1 and S100B-overexpressing mice at 1 month, t (10) = -2.272, p <0.05; 3 months, t (10) - 2.861, p < 0.02; and 6 months of age, t (10) = -3.441, p < 0.01 with S100B-overexpressing mice having significantly greater RAGE immunoreactivity than controls as shown in Fig 10. Within-subject ANOVA analysis of S100B mice suggested significant reactivity difference with age, F (3, 20) = 8.555, p = 0.001, specifically 6 month old animals had significantly greater reactivity than 1 and 12 month old animals, p < 0.005 and 3 month old animals, p < 0.05. No significant age differences were found within CD1 control animals, F (3, 20) = 0.486, p > 0.05 as shown in Fig 11.

RAGE post hoc analysis dentate gyrus

Independent *post hoc t*- test analysis of the upper blade of the dentate gyrus revealed greater RAGE reactivity in 6 month old S100B animals as compared to CD1 controls, t (10) = -3.212, $p < 0.01$. Within-subject ANOVA analysis of S100B mice suggested significant reactivity difference with age, F (3, 20) = 3.511, $p = 0.05$, specifically 6 month old animals had significantly greater reactivity than 1 month old animals, $p < 0.05$. No significant age differences were found within CD1 control animals, F (3, 20) = 0.431, $p > 0.05$.

Cresyl Violet Neuronal Density at 1, 3, 6 and 12 months of age

A 2 (Strain: CD1 or S100B) X 4 (Age: 1, 3, 6 or 12 months) repeated measures ANOVA revealed significant main effects of strain (Fig. 12) and age as well as a significant interaction of age x strain as shown in Table 5 for regions of interest including CA1 pyramidal, CA3 pyramidal and the upper blade of the dentate gyrus. No significant differences were found in the lower blade and hilus of the dentate gyrus. Average neuronal standardized optical density measurements for CD1 and S100B-overexpressing mice are shown in Table 6 for each age.

Table 5

Cresyl Violot Neuronal Density 2 X 4 Repeated Measures ANOVA for CD1 and S100B-overexpressing Animals at 1, 3, 6 and 12 Months of Age

Region of Interest	Effect/Interaction	Statistical Significance
CA1 pyramidal	Strain	$F(1, 10) = 51.827$, $p=0.00$*
	Age	$F(3, 30) = 59.309$, $p=0.00$*
	Age X Strain	$F(3, 30) = 36.578$, $p=0.00$*
CA3 pyramidal	Strain	$F(1, 10) = 25.284$, $p=0.001$*
	Age	$F(3, 30) = 79.403$, $p=0.00$*
	Age x Strain	$F(3, 30) = 35.616$, $p=0.00$*
Upper blade	Strain	$F(1, 10) = 0.122$, $p > 0.05$
Dentate gyrus	Age	$F(1, 30) = 84.708$, $p=0.00$*
	Age x Strain	$F(1, 30) = 2.00$, $p > 0.05$
Lower blade	Strain	$F(1, 10) = 0.254$, $p > 0.05$
Dentate gyrus	Age	$F(1, 30) = 7.603$, $p=0.001$*
	Age x Strain	$F(1, 30) = 0.088$, $p > 0.05$
Hilus	Strain	$F(1, 10) = 0.364$, $p > 0.05$
Dentate gyrus	Age	$F(1, 30) = 1.236$, $p > 0.05$
	Age x Strain	$F(1, 30) = 1.329$, $p > 0.05$

Note. * significance at $p < .005$; Sphericity Assumed

Table 6

Mean Cresyl Violet Neuronal Standardized Optical Density Measurements for CD1 and S100B-overexpressing Mice

Region of interest	Age (months)	Optical Density	Standard Deviation
CA1 pyramidal			
CD1	1	0.1509	0.0207
	3	0.3222	0.0304
	6	0.2996	0.0092
	12	0.3068	0.0126
S100B	1	0.1779	0.0207
	3	0.3487	0.0561
	6	0.2047	0.0341
	12	0.0880	0.0193
CA3 pyramidal			
CD1	1	0.1448	0.0144
	3	0.3215	0.0292
	6	0.2933	0.0124
	12	0.2900	0.0143
S100B	1	0.1740	0.0518
	3	0.3150	0.0293
	6	0.2670	0.0124
	12	0.0961	0.0456
Upper blade dentate gyrus			
CD1	1	0.1426	0.0188
	3	0.3177	0.0391
	6	0.2933	0.0124
	12	0.2900	0.0143
S100B	1	0.1772	0.0516
	3	0.3150	0.0254
	6	0.2804	0.0156
	12	0.2834	0.0156
Lower blade dentate gyrus			
CD1	1	0.2453	0.0235
	3	0.2909	0.0311
	6	0.2849	0.0152
	12	0.2884	0.0153
S100B	1	0.2439	0.0107
	3	0.2912	0.0321
	6	0.2804	0.0197
	12	0.2784	0.0227

Table 6 con't

Mean Cresyl Violet Neuronal Standardized Optical Density Measurements for CD1 and S100B-overexpressing Mice

Region of interest	Age (months)	Optical Density	Standard Deviation
Hilus dentate gyrus			
CD1	1	-0.0037	0.0213
	3	-0.0005	0.0206
	6	-0.0021	0.0278
	12	-0.0037	0.0207
S100B	1	0.0156	0.0465
	3	0.0073	0.0283
	6	0.0058	0.0303
	12	0.0003	0.0301

Note. Mean Standardized Optical Density if an average of n=6 per strain at each age for a total of N = 48 animals.

Cresyl Violet Neuronal Density post hoc analysis CA1 pyramidal

Independent *post hoc t*- test analysis of CA1 pyramidal revealed a significant difference between CD1 and S100B-overexpressing mice at 6 month, t (10) = 6.579, p = 0.00; and 12 months of age, t (10) = 23.302, p = 0.00 with S100B-overexpressing mice having significantly less neuronal density than controls. Within-subject ANOVA analysis of CD1 control mice suggested significant reactivity difference with age, F (3, 20) = 96.181, p = 0.00, specifically 1 month old animals had significantly less reactivity than 3, 6 and 12 month old animals, p = 0.00. S100B animals also had significant age associated neuronal density, F (3, 20) = 39.194, p = 0.00. However, 1 month old animals had significantly less reactivity than 3 and 6 month old animals but greater than 12 month old animals, $p < 0.01$. 3 month old animals also had significantly greater reactivity than all other ages, p = 0.00.

Cresyl Violet Neuronal Density post hoc analysis CA3 pyramidal

Independent *post hoc t*- test analysis of CA3 pyramidal revealed a significant difference between CD1 and S100B-overexpressing mice at 6 month, t (10) = 2.599, $p < 0.05$; and 12 months of age, t (10) = 9.956, p = 0.00 with S100B-overexpressing mice having significantly less neuronal density than controls as depicted in Fig 13. Within-subject ANOVA analysis of CD1 control mice suggested significant reactivity difference with age, F (3, 20) = 107.237, p = 0.00, specifically 1 month old animals had significantly less reactivity than 3, 6 month and 12 month old animals, p = 0.00 as depicted in Fig. 14. S100B animals also had significant age associated neuronal density, F (3, 20) = 38.955,

$p = 0.00$. 1 month old animals had significantly less reactivity than 3 and 6 month old animals but greater than 12 month olds, $p < 0.02$. 12 month old animals also had significantly less reactivity than all other ages, $p < 0.02$ as depicted in Fig. 15.

Cresyl Violet Neuronal Density post hoc analysis dentate gyrus

Within-subject ANOVA analysis of CD1 control mice $F(3, 20) = 68.329$, $p = 0.00$ and S100B animals $F(3, 20) = 22.726$, $p = 0.00$ suggested significant reactivity differences with age in the upper blade of the dentate gyrus in that 1 month old animals had significantly less reactivity than 3, 6 month and 12 month old animals, $p = 0.00$. Similar results were found in the lower blade of the dentate gyrus of CD1 control animals, $F(3, 20) = 5.587$, $p = 0.006$ with 1 month old animals having significantly less reactivity than 3, 6 month and 12 month old animals, $p < 0.05$.

Interaction of Microglia, RAGE and neuronal density at 1, 3, 6 and 12 months of age in CD1 and S100B-overexpressing mice

As shown in Table 7, neuronal cell body density is significantly dependent upon the interaction of the animal's age, microglia reactivity and RAGE expression. At 1 and 3 months of age, there are no significant differences in neuronal density between CD1 control and S100B-overexpressing mice within the CA1 and CA3 pyramidal region. However, at 1, 3 and 6 months of age, S100B-overexpressing mice have significantly greater RAGE reactivity than CD1 control animals. S100B mice also have significantly greater microglial reactivity than CD1 animals at 3, 6 and 12 months of age. As the S100B animal ages, the

microglial appear to be more in an activated as opposed to resting state as shown in Fig 5**.** Initially, S100B mice do not differ in neuronal cell body density from CD1 control animals although the RAGE expression is greater. As RAGE expression and age increases, microglial reactivity remains greater in the S100B strain. By 6 and 12 months of age, CD1 control animals have significantly greater neuronal density and less RAGE and microglia reactivity. Microglial reactivity in CD1 control animals appears to be in the resting as opposed to activated form as shown in Fig 4**.** At 12 months of age, S100B mice actually have decreased age-associated RAGE expression although microglial reactivity remains elevated. Because RAGE expression is found on neurons, the significant neuronal loss in 12 month old S100B animals may explain the resulting decreased RAGE expression although microglial reactivity remains elevated.

The basal dendritic region of CA1 and CA3 stratum oriens has greater microglial reactivity in S100B mice as opposed to CD1 control animals. As opposed to the pyramidal cell region of CA1 and CA3, the dendritic region appears to have the majority of microglia in the resting as opposed to activated state, although S100B animals express both transitional states. This would suggest resting microglia avoid areas containing neuronal cell bodies found in the pyramidal regions of the hippocampus and remain in the periphery of CD1 control animals. They appear mainly in the resting form in dendritic regions to perform monitoring functions in areas of synaptic connections. However, in S100B-overexpressing animals, microglial reaching the pyramidal cells bodies

appear mainly activated where neuronal density is decreased and remaining cell bodies express the highest concentration of the RAGE receptor for S100B.

Although no significant neuronal differences were found in the upper and lower blade of the dentate gyrus between CD1 and S100B animals, differences in microglia and RAGE reactivity were found. Within the upper blade, S100B mice had greater microglia reactivity at 6 and 12 months with greater RAGE expression at 6 months. The lower blade has significantly greater microglia expression only at 12 months of age.

The progression of damage in these mice appears to follow the highly predictable pattern of damage and neuronal loss associated with Alzheimer's disease (Schonheit et al., 2004), first spreading from the CA1 hippocampal subfield followed by the CA3 and eventually the dentate gyrus. Resting microglia cells in the dendritic region of stratum oriens of the CA1 and CA3 appear to transition to an activated morphology capable of invading the pyramidal neuronal cell body regions of CA1 and CA3, particularly within the S100B animals. Therefore, the degree of neuronal loss seen in these S100B animals appears to have a significant interaction of the presence of heightened RAGE expression coupled with microglial activation. The granule cells of the dentate gyrus appear to be following a similar pattern, but at a slower rate. Perhaps if animals were permitted at age longer, the dentate gyrus would undergo a similar rate of damage in S100B as compared to CD1 control animals.

Table 7

Summary of Significant Statistical Differences Between CD1 and S100B Mice

Region of interest	Age (months)	Microglia	RAGE	Neuronal Density
CA1 stratum oriens	1	-		
	3	+S		
	6	*S		
	12	*S		
CA1 pyramidal	1	-	+S	-
	3	*S	+S	-
	6	*S	+S	*C
	12	*S	-	*C
CA1 stratum radiatum	1	-		
	3	-		
	6	-		
	12	+S		
CA3 stratum oriens	1	*S		
	3	*S		
	6	+S		
	12	+S		
CA3 pyramidal	1	-	+S	-
	3	+S	+S	-
	6	*S	+S	+C
	12	*S	-	*C
CA3 stratum radiatum	1	-		
	3	-		
	6	-		
	12	-		
Upper blade	1	-	-	-
Dentate gyrus	3	-	-	-
	6	+S	+S	-
	12	*S	-	-
Lower blade	1	-	-	-
Dentate gyrus	3	-	-	-
	6	-	-	-
	12	*S	-	-
Hilus	1	-	-	
	3	-	-	
	6	-	-	
	12	-	-	

Note. *C: $p = 0.00$ with CD1 control animals having greater reactivity
*S $p = 0.00$ with S100B-overexpressing animals having greater reactivity
+C $p < 0.05$ with CD1 control animals having greater reactivity
+S $p < 0.05$ with S100B-overexpressing animals having greater reactivity

Results: Experiment 2a

Microglia Immunoreactivity

Significant differences in total microglia immunoreactivity of both resting and activated cells as determined by relative optical density and cells counts were found between the groups as shown in the representative photomicrograph of Fig. 16 depicting animals given the Vitamin E supplemented diet or control chow prenatally until 5.5 months of age.

When comparing total microglial immunoreactivity (Fig. 17) as determined by relative optical density measurements of both activated and resting cells combined, significant differences were found between the groups in CA1 stratum oriens, $F(3,12) = 14.255$, $p = 0.00$; in CA1 stratum radiatum, $F(3,12) = 8.319$, $p < 0.005$; CA3 stratum radiatum, $F(3,12) = 6.040$, $p < 0.02$ and the hilus, $F(3,12) = 10.910$, $p < 0.001$. No significant differences in total microglial optical densities were found in the hippocampal areas of CA1 pyramidal cells, CA3 stratum oriens, and CA3 pyramidal cells, $p > 0.05$.

Post hoc analysis of CA1 stratum oriens revealed S100B Vitamin E diet animals (SE) had greater average relative optical density measurements than either CD1 Vitamin E (CE) diet animals $p = 0.00$ and CD1 control diet (CC) animals $p < .03$. S100B control (SC) diet animals also had greater immunoreactivity than CE diet animals, $p < 0.005$. CA1 stratum oriens results are shown in Fig. 17A. Bonferroni analysis of CA1 stratum radiatum revealed greater average immunoreactivity between SE animals versus CE animals, $p = 0.003$ and SC animals as compared to CE animals, $p < 0.05$ as shown in Fig. 17B**.**

Bonferroni analysis of the CA3 stratum radiatum region of the hippocampus revealed SE animals had greater optical density values than CE diet animals, $p < 0.01$ as shown in Fig. 17C. *Post hoc* analysis of the hilus as shown in Fig. 17D revealed greater average optical density values in the SE animals as compared to the CE diet animals, $p = 0.001$ and the CC animals, $p < 0.05$.

When comparing only the number of activated microglia cells (Fig. 18), significant differences were found in the CA1 pyramidal region of the hippocampus $F(3, 12) = 5.213$, $p < .02$. *Post hoc* analysis revealed that S100B animals on a Vitamin E supplemented diet (5.00 +/- 3.16) had on average significantly more reactive microglia than either the SC animals (0.75 +/- 0.96), the CE diet animals (0.75 +/- 1.5) and the CC diet animals (0.71 +/- 0.89), $p < 0.005$ as shown in Fig. 18A. Similar results were also found in the CA1 stratum oriens region of the hippocampus, $F(3, 12) = 11.977$, $p = 0.001$ as shown in Fig. 18B. Again, S100B animals on the Vitamin E diet (6.58 +/- 2.50) had on average significantly more activated microglia cells than S100B control diet animals (1.13 +/- 1.03), CD1 Vitamin E diet animals (0.92 +/- 1.83) and CD1 control diet animals (0.63 +/- 0.48), $p < 0.005$. No significant differences in activated microglia were found in the hippocampal regions of CA1 stratum radiatum, CA3 stratum orien, CA3 stratum radiatum, CA3 pyramidal or the hilus.

Therefore, S100B animals on a Vitamin E diet appear to have more total microglial cells within the basal and apical dendritic regions of CA1 stratum oriens and radiatum respectively, as opposed to the pyramidal cell regions. In

contrast, the pyramidal cell regions of CA1 appear to have more activated as opposed to total microglial cell counts. Because the total cell count includes resting and activated forms, this would suggest resting microglia avoid areas containing neuronal cell bodies found in the pyramidal regions of the hippocampus and remain in the periphery. They appear mainly in the resting form in dendritic regions to perform monitoring functions in areas of synaptic connections. Although CA1 stratum radiatum includes a higher total count of cells, the majority has not yet transitioned to an activated state. Microglial reaching the pyramidal cells bodies appear mainly activated where cell bodies express the highest concentration of the RAGE receptor for S100B.

More strikingly, the CD1 animals on the Vitamin E diet appear to have a slight yet non-significant decrease in total microglia cell counts as compared to those on the control diet. This suggests that the effects of Vitamin E have a dependence on the presence of heightened levels of S100B and the RAGE receptor. In typical brain, the supplementation of Vitamin E appears to decrease the amount of neuroinflammation as determined by microglial activation. However, in a brain already susceptible to inflammatory processes with heightened S100B and RAGE, Vitamin E was shown to increase the activation of cells, particularly within the CA1 pyramidal region. The potential neuroprotective and neurotoxic functions of these finding will be addressed in Experiement 2b through neuronal density measurements.

RAGE Immunoreactivity

Significant differences in RAGE relative optical density were found in the CA1 pyramidal cell region of the hippocampus between the strain and dietary groups, $F(3, 12) = 29.118$, $p = 0.00$ but not in the CA3 pyramidal region $F(3,12) = .979$, $p > 0.5$. *Post hoc* analysis of the CA1 pyramidal region revealed S100B animals on the Vitamin E supplemented diet had significantly greater average RAGE relative optical density values than all other groups, $p < 0.002$ as shown in Fig. 19**.**

Significant differences in RAGE immunoreactivity are only seen within the CA1 but not CA3 pyramidal region or within apical and basal dendritic regions of the stratum oriens and radiatum. The higher level of RAGE in the pyramidal as opposed to dendritic regions can be explained by the fact that RAGE is localized on neuronal cell bodies as well as microglia. Neuronal cell bodies are the predominant structures in the pyramidal layer as opposed to dendrites in the stratum oriens and radiatum. Higher numbers of cell bodies in this region would lead to a greater expected RAGE level in comparison to dendritic regions, regardless of microglia cell presence. However, RAGE levels are expected to be higher overall in both pyramidal and dendritic regions in the S100B over-expressing mice. Therefore, as opposed to the CA1 stratum oriens, the pyramidal region contains the highest concentration of RAGE as well as activated microglial cells are within the S100B over-expressing animals. Although the direct mechanism is not known, further support for the influence of RAGE activating microglia is the occurrence of higher levels of RAGE

immunopositive cells in CA1 but not CA3 pyramidal regions. The CA1 region was already shown to have significantly more activated microglia cells whereas CA3 was not. Before any conclusions can be drawn in regard to neuronal toxicity induced by Vitamin E in S100B-overexpressing animals, cresyl violet neuronal density measurements would need to be conducted as explained in Experiment 2b.

Results: Experiment 2b

Microglia Immunoreactivity

Significant differences in total microglia immunoreactivity of both resting and activated cells as determined by standardized optical density measurements were found between the groups as shown in the representative photomicrograph of Fig. 20 of animals given the Vitamin E supplemented diet as compared to the control diet from 5.5 -10 months of age as compared to a control diet.

When comparing total microglial immunoreactivity as determined by standardized optical density measurements of both activated and resting cells combined, significant differences were found in all regions of interest of CA1 (Fig 21), CA3 (Fig. 22) and dentate gyrus (Fig. 23) including CA1 stratum oriens, $F(3, 12) = 52.61$, $p = 0.00$; pyramidal, $F(3, 12) = 104.98$, $p = 0.00$; and stratum radiatum $F(3, 12) = 375.31$, $p = 0.00$; CA3 stratum oriens, $F(3, 12) = 196.12$, $p = 0.00$; pyramidal region, $F(3, 12) = 92.28$, $p = 0.00$; stratum radiatum, $F(3, 12) = 37.52$, $p = 0.00$; as well as the upper, $F(3, 12) = 80.11$, $p = 0.00$ and lower blades, $F(3, 12) = 178.10$, $p = 0.00$ and hilus $F(3, 12) = 150740$, $p = 0.00$ of the dentate gyrus.

Bonferroni Post hoc analysis of CA1 microglia

Post hoc analysis of CA1 stratum oriens revealed S100B Vitamin E diet animals (0.0290 +/- 0.0049) had significantly greater total microglial immunoreactivity that all other groups (CC 0.0101 +/- 0.0001; CE 0.0100 +/- 0.000, SC 0.0158 +/- 0.0002), $p = 0.00$. S100B control diet animals also expressed significantly greater reactivity that CD1 animals on either diet, $p < 0.05$. *Post hoc* analysis of CA1 pyramidal region revealed each group was significantly different from all other groups (SE 0.0566 +/- 0.0023, SC 0.0422 +/- 0.0023, CE 0.0191 +/- 0.0061, CC 0.0010 +/- 0.0001) $p < 0.05$. *Post hoc* analysis of CA1 stratum radiatum revealed S100B Vitamin E (0.0213 +/- 0.0000) animals has significantly greater immunoreactivity than all other groups (SC 0.0113 +/- 0.0000; CE 0.0104 +/- 0.0004; CC 0.0131 +/- 0.000), $p = 0.00$. CD1 control diet animals had significantly greater reactivity than CD1 Vitamin E and S100B control diet animals, $p < 0.01$.

Bonferroni Post hoc analysis of CA3 microglia

Post hoc analysis of CA3 stratum oriens revealed all groups were significantly different from each other (SE 0.0364 +/- 0.0017, SC 0.0194 +/- 0.0005, CE 0.0100 +/- 0.0000, CC 0.0147 +/- 0.0028) $p < .05$. *Post hoc* analysis of CA3 pyramidal again revealed all groups were significantly different from each other with S100B Vitamin E (0.0596 +/- 0.0005) having the greatest immunoreactivity followed by S100B control (0.0400 +/- .0088), CD1 Vitamin E (0.0238 +/- 0.0050) and CD1 control (0.0183 +/- 0.0011), $p < 0.05$. *Post hoc* analysis of CA3 stratum radiatum revealed that S100B Vitamin E (0.0295 +/-

.0005) animals had significantly greater microglial immunoreactivity than all other groups (S100B control 0.0119 +/- 0.0038, CD1 Vitamin E .0075 +/- .0050, CD1 control 0.0127 +/- .0006), $p < 0.05$.

Bonferroni Post hoc analysis of dentate gyrus microglia

Post hoc analysis of the upper blade of the dentate gyrus revealed CD1 control animals (0.0002 +/- 0.0001) had significantly less immunoreactivity than all other groups (CE 0.0012 +/- 0.0000, SC 0.0013 +/- 0.0001, SE 0.0012 +/- 0.0001) $p < 0.05$. *Post hoc* analysis of the lower blade of the dentate gyrus revealed S100B Vitamin E (0.0063 +/- 0.0004) diet animals had significantly greater immunoreactivity than all other groups (SC 0.0013 +/- 0.0000, CE 0.0013 +/- 0.0007, CC 0.0002 +/- 0.0001), $p = 0.00$. CD1 control diet animals had significantly less immunoreactivity than all other groups, $p < 0.05$. Post hoc analysis of the hilus revealed CD1 control animals (0.0124 +/- 0.0000) had significantly greater immunoreactivity than all other groups (CE 0.0001 +/- 0.000, SC 0.0001 +/- 0.0000, SE 0.0001 +/- 0.000) $p = 0.00$.

RAGE Immunoreactivity

Significant differences in RAGE standardized optical density measurements were found in the CA1 pyramidal, $F (3, 12) = 14.31$, $p = 0.00$; CA3 pyramidal, $F (3, 12) = 7.85$, $p = 0.004$ and lower blade of the dentate gyrus, $F (3, 12) = 8.17$, $p = 0.003$ as shown in Fig. 24.

Bonferroni Post hoc analysis RAGE

Post hoc analysis of CA1 pyramidal revealed CD1 control animals (0.0104 +/- 0.0075) had significantly greater RAGE immunoreactivity than all other groups (CE -0.0199 +/- 0.0089, SC -0.0275 +/- 0.0122, SE -0.0162 +/- 0.0044), $p = 0.00$. *Post hoc* analysis of CA3 pyramidal region revealed that CD1 control animals (-0.0125 +/- 0.0050) had significantly greater RAGE immunoreactivity than CD1 Vitamin E (-0.0423 +/- 0.0003) and S100B control animals (-0.0487 +/- 0.0171) but not S100B Vitamin E animals (-0.0342 +/- 0.0017), $p < 0.05$. *Post hoc* analysis of the lower blade of the dentate gyrus revealed CD1 control animals (-0.0075 +/- 0.0050) had significantly greater immunoreactivity than S100B Vitamin E animals (-0.0575 +/- 0.0096) $p = 0.003$.

Cresyl Violet Neuronal Density

Signficant differences in cresyl violet neuronal density measurements were found in all regions of interest including CA1 pyramidal, $F (3, 12) = 23.10$, $p = 0.00$; CA3 pyramidal $F (3, 12) = 15.48$, $p = 0.00$; upper blade of the dentate gyrus $F (3, 12) = 50.75$, $p = 0.00$; and lower blade of the dentate gyrus $F (3, 12) = 70.71$, $p = 0.00$ as shown in Fig. 25.

Bonferroni Post hoc analysis neuronal density

Post hoc analysis of CA1 pyramidal region revealed that CD1 control animals (0.0658 +/- 0.0158) had significantly greater neuronal optical density measurements than CD1 Vitamin E (0.0492 +/- 0.0284), S100B Vitamin E (-0.0562 +/- 0.0253) and S100B control animals (0.0166 +/- 0.0056), $p < 0.05$. S100B Vitamin E animals had significantly less neuronal density staining than all

other groups, $p < 0.005$. *Post hoc* analysis of CA3 pyramidal revealed that CD1 control animals (0.0583 +/- 0.0495) had significantly greater neuronal density than CD1 Vitamin E (-0.0283 +/- 0.0221), S100B Vitamin E (-0.0790 +/- 0.0218) and S100B control diet animals (0.0100 +/- 0.0120), $p < 0.05$. S100B Vitamin E animals had significantly less neuronal density than CD1 control or S100B control diet animals, $p < 0.05$. Within the upper blade of the dentate gyrus, S100B Vitamin E (-0.0725 +/- 0.0171) had significantly less neuronal immunoreactivity than S100B control (0.0600 +/- 0.0082), CD1 control (0.0725 +/-0.0250) and CD1 Vitamin E (0.0050 +/- 0.0173), $p < 0.005$. CD1 Vitamin E also had significantly less neuronal density than CD1 control and S100B control diet animals, $p < 0.005$. Within the lower blade of the dentate gyrus, a similar pattern was found with significantly less neuronal density in S100B Vitamin E animals (-0.0781 +/- 0.0135) compared to S100B control (0.0617 +/- 0.0042), CD1 Vitamin E (0.0050 +/- 0.0174) and CD1 control diet animals (0.0643 +/- 0.0147), $p < 0.005$. CD1 Vitamin E animals had significantly less neuronal density than CD1 control and S100B control diet animals, $p < 0.005$.

Overall, S100B animals on the Vitamin E supplemented diet had significantly greater microglial reactivity than S100B control diet mice or either group of CD1 control animals. Within the region of apical dendrites of stratum oriens, the S100B animals on the Vitamin E diet appear to have more microglial cells in the activated form whereas reactivity of CD1 animals appear to be mainly in the resting morphology. Within the pyramidal and granule cell regions, S100B Vitamin E animals again have the highest level of reactivity in the activated form.

However, CD1 animals on a control diet have significantly greater RAGE expression as compared to other groups in the pyramidal and granule cell regions. This may be explained by the fact that the CD1 control animals have the highest intensity of neuronal staining which can also express the RAGE receptor. CD1 control animals have the greatest intensity of microglial reactivity in the hilus of the dentate gyrus, but all cells appear in the resting form. It appears that these animals also follow the pattern of neuronal loss associated with Alzheimer's disease. By 10.5 months of age, S100B mice, particularly on the Vitamin E diet, have significant neuronal loss within CA1 and CA3 pyramidal regions and granule cells of the dentate gyrus associated with decreased RAGE expression and increased microglial reactivity.

Discussion

The current study looks at the effects of age associated chronic S100B-overexpression on the reactivity of microglial cells, RAGE receptor upregulation and neuronal cell density as well as the role of the antioxidant Vitamin E during development and aging.

The findings from Experiments 1, 2a and 2b can be summarized as follows: The receptor for S100B, RAGE, can be co-localized on neurons as well as activated microglial cells as is shown by double-labeling immunocytochemistry. S100B-overexpressing transgenic mice display increases in microglia cell immunoreactivity with aging from 1, 3, 6 until 12 months of age as compared to CD1 control mice. These cells also appear to have an increase

in transition from a resting and ramified morphology to an activated and ameboid shaped morphology as the animal ages. S100B mice also have an increase in RAGE upregulation as the animal ages until a decline in RAGE reactivity is seen by 12 months of age. Because the RAGE receptor can be localized to neurons as well as glia, this decrease in RAGE expression can possibly be attributed to the increased neuronal loss of S100B-overexpressing transgenic mice with age.

At 1 month of age, S100B mice have greater RAGE reactivity although there are no differences in microglial immunoreactivity or neuronal density as compared to CD1 control animals. By 3 months of age, S100B mice continue to have elevated RAGE expression but accompanied with increases in microglial reactivity although neuronal density remains equal to that of CD1 animals. At six months of age, S100B mice have elevated RAGE and microglial reactivity as well as neuronal loss as compared to CD1 controls. By 12 months, S100B mice continue to have elevated microglial reactivity, but decreased RAGE expression with severe neuronal loss.

Therefore, it appears RAGE upregulation begins in S100B mice prior to the onset of microglial activation and neuronal loss. However, once neuronal loss is sufficient and RAGE expression decreases, microglial staining intensity remains elevated. This pattern of damage is greatest in the CA1 and CA3 pyramidal regions followed by the granule cells of the dentate gyrus consistent of the pattern of damage associated with Alzheimer's disease. Within the dendritic regions, microglial activation is greatest in the resting form, although some cells appear activated within S100B mice.

In an attempt to mediate S100B-overexpression induced RAGE upregulation and microglial activation, the antioxidant DL-alpha tocopheryl acetate (Vitamin E) was given as a dietary supplement during either development or aging. However, Vitamin E significantly increased microglial activation is S100B mice when given prenataly until 5.5 months of age and from 5.5 months until 10 months of age. With early dietary Vitamin E supplementation, RAGE expression was also significantly increased in S100B-overexpressing animals as compared to controls on either diet. Later dietary supplementation of Vitamin E did not create a significant increase in RAGE expression in S100B animals. CD1 control animals had the greatest expression of RAGE receptor reactivity. This may be due to the significant neuronal loss associated with the Vitamin E diet in both animal strains, with the most severe neuronal loss found in S100B-overexpressing animals on the Vitamin E diet. CD1 control animals on a control diet maintain the highest level of neuronal cell body density. Although CD1 animals have increases in microglial reactivity associated with the Vitamin E diet, they appear to remain in the resting morphology.

Therefore, within the S100B-overexpressing transgenic mouse, Vitamin E appears to increase microglial reactivity and activation, RAGE upregulation and neuronal loss. Vitamin E supplementation in a CD1 control mouse appears to increase microglial reactivity, but they remain in a resting and ramified morphology. Cell loss is still evident in CD1 Vitamin E animals although not as severe as with the S100B transgenic mouse.

In the brain, S100B, a member of the S100 superfamily of calcium binding proteins, is produced by astroglial cells and specifically released into the neuropil in response to a number of neurochemical factors including serotonin (Whitaker-Azmitia, et al., 1989; Whitaker-Azmitia et al., 1990) tissue insults or trauma (Anderson et al., 2001; Cotena et al., 2006) and ischemia (Parker et al., 1998; Rothermundt, et al., 2003) and decreased release by glutamate (Tramontina et al., 2006). Although predominantly expressed by astroglia, S100B can also be expressed at much lower levels in microglia (Adami et al., 2001), radial glia (Castagna et al., 2003) and oligodendrocytes (Richter-Landsberg & Heinrich, 1995). Developmental studies involving the role of S100B have demonstrated age-related changes in S100B tissue expression and distribution in the CNS of mammals which may be related to the different roles of this protein in distinct brain regions throughout the lifespan (Tiu et al., 2000; Donato, 2001). S100B levels peak in neonatal mammals at a level almost tenfold that seen in adulthood, decrease, and then increase again in aged animals with particularly heightened levels with pathological aging such as AD and DS (Griffin et al., 1989; Lott & Head, 2001; Portela et al., 2002). Extracellular functions of the S100B protein in the aged brain include apoptosis (Mariggio et al., 1994, Shapiro et al., 2004), pathogen recognition, glial proliferation, and neuroinflammatory responses (Griffin et al, 1989; Akiyama et al., 1994; Li et al., 2000). In the immature brain, S100B promotes cortical neurite growth, serotonin terminal development and synaptogenesis (Azmitia et al., 1990).

As is apparent with S100B, a protein with a variety of extracellular effects must be strictly regulated *in vivo*. The extracellular effects of S100B vary with tissue concentration (Kligman & Marshak, 1985; Van Eldik et al., 1988; Barger et al., 1992; Donato, 2001), age of the brain (Rothermundt, et al., 2003), and physicochemical state of the protein itself (Zimmer et al., 1995) such as being bound by calcium, dimerization (Baudier, et al., 1984; Landar et al., 1997; Smith & Shaw, 1998a/b; Donato, 2001) and oxidation state of the protein (Winningham-Major et al., 1989; Scotto et al., 1998; Goncalves et al., 2000; Koppal et al., 2001; Zhukova et al., 2004).

As shown by the effects of the antioxidant Vitamin E, the oxidation state of the S100B protein is important for regulating these extracellular effects. While the oxidation of the cysteine residues of S100B is necessary for the neurotrophic characteristics and mitogenic effects on astrocytes, S100B proteins that lack one or both of the cysteine residues are capable of inducing inflammatory responses in microglia (Koppal et al., 2001). Although the two cysteine residues are not necessary for the noncovalent dimerization of S100B, they are important in S100B target protein interactions (Landar et al., 1997). S100B exists mainly as a homodimer with each subunit containing two calcium binding domains flanked by N- and C- terminal helices (Drohat et al., 1996; Kilby et al., 1996; Smith & Shaw, 1998a/b). Those proteins lacking one or both cysteines residues display no neurotrophic activities (Winningham-Major et al., 1989) while the form lacking both residues can induce glial activation responses in the form of iNOS and IL-1β production (Koppal et al., 2001). Therefore, the structural features of S100B that

are necessary for neurotrophic effects may be distinct from those related to its glial activation responses. Although not directly assessed by this study, Vitamin E may be one mechanism involved in this structural switch in oxidation state and pathway change from one of neuronal survival to one of inflammatory response generation in animals over-expressing the S100B protein. These S100B level increases coupled with a potential change in oxidation state could lead to the cellular changes of neuroinflammation characterized by microglial activation with increased pro-inflammatory markers (Streit, Mrak, & Griffin, 2004). Further evidence for this tight regulatory influence of glial environment is demonstrated when high glucose inhibits S100B release (Nardin et al., 2007). Those astrocytes cultured in high glucose medium displayed an atypical morphology, reduced proliferation, and a reduced amount of extracellular S100B production. If the S100B protein is in the favorable oxidized form, this decrease in production could negatively affect neuronal activity and survival or a change in structural form could induce an inflammatory response.

In addition to the oxidation state of the protein, the extracellular effects of S100B are regulated in part by the expression levels of RAGE on neurons and glia. Relatively low levels of RAGE expression are found in typical tissue, but with high levels of its ligands such as S100B, beta amyloid, and AGE's (advanced glycation endproducts), RAGE expression increases (Schmidt et al., 2000). This can be seen in the CA1 region of the hippocampus of S100B-overexpressing animals on both the control diet, but particularly with the Vitamin E supplemented diet given to younger animals. S100B/RAGE interactions may then lead to

inflammatory processes causing pathological changes in microglial cells (Bianchi et al., 2007). Stimulation of RAGE on microglial cells causes release of free radicals (Huttunen et al., 2000) and increased generation of superoxide (O2-) in mononuclear phagocytes (Ding et al., 2007). Our results with RAGE immunodensitometry would suggest from a neurotoxic viewpoint that predominantly unoxidized S100B via Vitamin E supplementation increases RAGE expression, since the greatest amount of RAGE expression occurs in those S100B animals treated chronically with Vitamin E.

Increased brain oxidative stress in the form of lipid peroxidation and neuroinflammatory processes are also key features of pathological aging (McGeer et al., 1987; Rogers et al., 1988; Smith et al., 2000). The brain's high oxygen consumption rate and concentration of oxidizable lipids and transition metal ions capable of producing reactive oxygen species leave it especially vulnerable to oxidative stress (Spector et al., 1977; Bush, 2000; Kontush et al., 2001; Kontush et al., 2004). The non-reducing conditions of the extracellular space favor oxidation of S100B (Sen & Belli, 2007) which may result in a structural change (Zhukova et al., 2004). Thus, as the brain ages or is exposed to trauma, more and more of the S100B would be in the oxidized state. It is apparently the oxidized state which increases the neurotrophic potential as the neurotrophic effects of S100B appear to depend on a disulfide-linked dimeric form while the reduced form has no neurite extension inducing activity (Winningham-Major et al., 1989). Our results therefore suggest that the reduced state of S100B is related to the neuroinflammatory processes – since treatment

with the antioxidant Vitamin E increased microglial activation. More activated microglia suggests greater neuroinflammatory processes are occurring. In future studies, it may be worthwhile to determine whether or not the reduced state of S100B is a direct result of a Vitamin E supplemented diet. This would suggest a neurotoxic role of microglial activation through a negative feedback regulatory pathway. S100B typically releases free radicals, which oxidizes S100B and prevents further stimulation of the RAGE receptor since oxidized S100B typically is neurotrophic and protective. However, treatment with an antioxidant to an animal already over-expressing S100B may interrupt this feedback leading to further increases in RAGE upregulation and glial activation. In the current study, microglial activation and RAGE expression were most evident in the CA1 and CA3 pyramidal regions and longer treatment times may have shown the same regional progression of damage as is seen in AD.

As an alternative explanation, it is possible that the increases in microglial activation and RAGE upregulation is beneficial. A potentially neuroprotective mechanism may be occurring with Vitamin E supplementation in CD1 animals given the diet at a younger age by maintaining the endogenous CNS immune function. Cell culture studies of rat microglial cells given Vitamin E show a dramatic induction of microglial proliferation and ramification with decreased production of pro-inflammatory IL-1β (Flanary & Streit, 2006; Heppner et al., 1998). Therefore, it is important to determine whether increases in activated microglial cells actually display pro-inflammatory markers or if they potentially

have a beneficial role. An increase in activation number may not necessarily mean more damage is occurring.

As previously mentioned, chronic attempts of microglia to clear neuronal damage, possibly caused by Aβ deposition or heightened levels of S100B, result in a cycle of neuroinflammatory processes. This would eventually lead to a senescence and deterioration of microglia cells and loss of their neuroprotective function (Akiyama et al., 2000; McGeer & McGeer, 2001; Rogers et al., 2002; Streit, 2004; Block et al., 2007). Because microglia cells are the only mature cells capable of undergoing mitosis, they may have a need for self-renewal due to a limited lifespan (Graeber at al., 1988; Streit, 2004) with renewal capacity limited with aging. Supplementation of Vitamin E that increases microglial activation may maintain the ability of glia to degrade harmful proteins in a beneficial manner that is typically decreased in aging brains. As shown by cell culture of isolated microglia cells, the inability of permanently activated cells from adult animals to degrade extracellular material successfully was partially overcome by Vitamin E supplementation (Stolzing et al., 2006).

In a typical CD1 control animal, Vitamin E may be neuroprotective in maintaining a stable and homeostatic neuronal environment where large numbers of microglia cells capable of transitioning to an activated form are not needed. Although not significantly different, CD1 control animals appeared to have an overall decrease in total microglia immunoreactivity when given the diet at a young age as opposed to later in life. This is supported by previous work showing that microglia cells treated with Vitamin E in culture showed a decrease

in pro-inflammatory products including interleukin-1α and TNFα (Li et al., 2001). Without the presence of elevated S100B, heightened levels of microglia immunoreactivity would not be necessary and Vitamin E helps to maintain a stable anti-inflammatory environment.

Finally, this study shows the importance of knowing the underlying etiology before choosing a treatment. For example, DS (which includes a triplication of S100B susceptible to state reduction) and high probability of developing AD, Vitamin E may not be a method of choice without knowing the direct underlying mechanism of the antioxidant on both S100B and glial cells. Introducing an antioxidant into an environment susceptible to inflammatory responses as opposed to neurotrophic activity would not be favorable. Perhaps in DS, the high levels of S100B throughout development coupled with the increased in RAGE and microglial activation have a negative inflammatory response when an antioxidant capable of state change in this protein is introduced. Although low levels of extracellular S100B in an oxidized state is able to enhance neuronal activity and survival, introducing an antioxidant to an environment of over-expression may provide a pathway of increased neuroinflammation.

In future studies, we will need to assess the direct effects of Vitamin E on determining the oxidized or reduced state of the S100B protein. It would also be necessary to determine whether these increases in microglia activation demonstrate a neuroinflammatory mechanism including production of pro-inflammatory markers such as IL-1β and COX-2 and determining neuronal loss

when giving the diet as a preventative at a young age as opposed to a treatment in older animals. Just as importantly, it should be determined whether this activation increase is beneficial in maintaining the endogenous immune system of the brain in an uncompromised organism such as the CD1 control mouse as compared to the S100B-overexpressing transgenic. Perhaps at a younger age, Vitamin E is beneficial for maintaining the endogenous immune system in a control mouse but harmful in an already compromised state.

Bibliography

Adami C, Guglielmo S, Blasi E, Agneletii A L, Bistoni F, Donato R. 2001. S100B expression in and effects on microglia. *Glia* 33(2): 131-142.

Akiyama H, Barger S, Barnum S, Bradt B, Bauer J, Cole GM. 2000. Inflammation and Alzheimer's disease. *Neurobiology of Aging* 21: 383-421.

Anderson RE, Hansson LO, Nilsson O, Dijlai-Merzoug R, Settergren G. 2001. High serum S100B levels for trauma patients without head injuries. *Neurosurgery* 48(6): 1255-1280.

Austyn JM, Gordon S. 1981. F4/80, a monoclonal antibody directed specifically against the mouse macrophage. *European Journal of Immunology* 11: 805-815.

Barger SW, Wolchok SR, Van Eldik LJ. 1992. Disulfide-linked S100 beta dimers and signal transduction. *Biochim Biophys Acta* 1160(1):105-112.

Baudier J, Glasser N, Haglid K, Gerard D. 1984. Purification, characterization and ion binding properties of human brain S100b protein. *Biochim Biophys Acta* 790(2): 164-173.

Bell K, Shokrian D, Potenzieri C, Whitaker-Azmitia PM. 2003. Harm avoidance, anxiety, and response to novelty in the adolescent S-100beta transgenic mouse: role of serotonin and relevance to Down syndrome. *Neuropsychopharmacology* 28(10): 1810-1816.

Bianchi R, Adami C, Giambanco I, Donato R. 2007. S100B binding to RAGE in microglia stimulates COX-2 expression. *Journal of Leukocyte Biology* 81(1): 108-118.

Block ML, Zecca L, Hong JS. 2007. Microglia-mediated neurotoxicity: uncovering the molecular mechanisms. *Nature Reviews Neuroscience* 8(1):57-69.

Bush AI. 2000. Metals and neuroscience. *Current Opinion in Chemical Biology* 4: 184-191.

Cagnin A, Brooks DJ, Kennedy AM, Gunn RN, Myers R, Turkheimer FE. 2001. *In vivo* measurement of activated microglia in dementia. *Lancet* 358: 461-467.

Castanga C, Viglietti-Panzica C, Panzica GC. 2003. Protein S100 immunoreactivity in glial cells and neurons of the Japanese quail brain. *Journal of Chemical Neuroanatomy* 25(3): 195-212.

Cotena S, Piazza O, Storti M. 2006. The S100B protein and traumatic brain injury. *Journal of Neurosurgery* 104(6 Suppl): 435-460.

Ding Y, Kantarci A, Hasturk H, Trackman PC, Malabanan A, Van Dyke TE 2007. Activation of RAGE induces elevated O2- generation by mononuclear phagocytes in diabetes. *Journal of Leukocyte Biology* 81(2): 520-527.

DiPatre PL, Gelmann BB. 1997. Microglial cell activation in aging and Alzheimer disease: partial linkage with neurofibrillary tangle burden in the hippocampus. *Journal of Neuropathology and Experimental Neurology* 56(2): 143-149.

Domanska-Janik K, Bronisz-Kowalczyk A, Zajac H, Zablocka B. 2001. Interrelations between nuclear-factor kappa B activation, glial response and neuronal apoptosis in gerbil hippocampus after ischemia. *Acta Neurobiol Exp (Wars), 61*(1), 45-51

Donato R. 2001. Functional roles of S100 proteins, calcium-binding proteins of the EF-hand type. *Biochemica Biophysica Acta* 1450:191-231.

Donato, R. 2007. RAGE: a single receptor for several ligands and different cellular responses: the case of certain S100 proteins. *Current Molecular Medicine* 7(8): 711-725.

Drache B, Diehl GE, Beyreuther K, Perlmutter LS, König G. 1997. Bcl-xl-specific antibody labels activated microglia associated with Alzheimer's disease and other pathological states. *Journal of Neuroscience Research* 47(1): 98-108.

Drohat AC, Amburgey JC, Abildgaard F, Starich MR, Baldisseri D, Weber DJ. 1996. Solution structure of rat apo-S100B (beta) as determined by NMR spectroscopy. *Biochemistry* 35: 11577-11588.

Flanary BE, Streit WJ. 2006. Alpha-tocopherol (vitamin E) induces rapid, nonsustained proliferation in cultured rat microglia. *Glia* 53(6): 669-74.

Frackowiak J, Wisniewski HM, Wegiel J, Merz GS, Iqbal K, Wang KC. 1992. Ultrastructure of the microglia that phagocytose amyloid and the microglia that produce beta-amyloid fibrils. *Acta Neuropathol* 84(3): 225-33.

Friend WC, Clapoff S, Landry C, Becker LE, O'Hanlon D, Allore RJ, Brown IR, Marks A, Roder J, Dunn RJ. 1992. Cell specific expression of high levels of human S100β in transgenic mouse brain is dependent on gene dosage. *Journal of Neuroscience* 12*:* 4337-4346.

Gerlai R, Marks A, & Roder J. 1994. T-maze spontaneous alternation rate is decreased in S100 beta transgenic mice. *Behavioral Neuroscience* 108(1): 100-106.

Gerlai R, Roder J. 1995. Abnormal exploratory behavior in transgenic mice carrying multiple copies of the human gene for S100 beta. *Journal of Psychiatry & Neuroscience* 20(2): 105-112.

Gerlai R, Roder J. 1996. Spatial and nonspatial learning in mice: effects of S100 beta overexpression and age. *Neurobiology of Learning & Memory* 66(2): 143-154.

Goncalves DS, Lenz G, Karl J, Goncalves CA, Rodnight R. 2000. Extracellular S100B protein modulates ERK in astrocytes cultures. *NeuroReport* 11: 807-809.

Graeber MB, Tetzlaff W, Streit WJ, Kreutzberg GW. 1988. Microglial cells but not astrocytes undergo mitosis following rat facial nerve axotomy. *Neuroscience Letters* 85(3): 317-321.

Griffin WS, Sheng JG, McKenzie JE, Royston MC, Gentleman SM, Brumback RA, Cork LC, Del Bigio MR, Roberts GW, Mrak RE. 1998a. Life-long overexpression of S100beta in Down's syndrome: implications for Alzheimer's pathogenesis. *Neurobiology of Aging.* 19(5): 401-405.

Giffin WS, Sheng JG, Royston MC, Gentleman SM, McKenzie JE, Graham DI, Roberts GW, Mrak RE. 1998b. Glial-neuronal interactions in Alzheimer's disease: the potential role of a 'cytokine cycle' in disease progression. *Brain Pathology* 8(1): 65-72.

Griffin WS, Stanley LC, Ling C, White L, MacLeod V, Perrot LJ, White CL 3rd, Araoz C. 1989. Brain interleukin 1 and S-100 immunoreactivity are elevated in Down syndrome and Alzheimer's disease. *Proceedings of the National Academy of Sciences USA* 86(19): 7611-7615.

Grundman M, Grundman M, Delaney P. 2002. Antioxidant strategies for Alzheimer's disease. *Proceedings of the Nutrition Society* 61(2): 191-202.

Haslbeck KM, Bierhaus A, Erwin S, Kirchner A, Nawroth P, Schlotzer U, Neundorfer B, Heuss D. 2004. Receptor for advanced glycation endproduct (RAGE)-mediated nuclear factor-kappaB activation in vasculitic neuropathy. *Muscle and Nerve, 29*(6), 853-860.

Heppner FL, Roth K, Nitsch R, Hailer NP. 1998. Vitamin E induces ramification and downregulation of adhesion molecules in cultured microglial cells. *Glia* 22(2): 180-188.

Hofmann MA, Drury S, Caifend F, Qu W, Taguchi A, Lu Y, Avila C, Kambham N, Bierhaus A, Nawroth P, Neurath MF, Slattery T, Beach D, McClary J, Nagashima M, Morser J, Stern D, Schmidt AM. 1999. RAGE mediates a novel proinflammatory axis: a central cell surface receptor for S100/calgranulin polypeptides. *Cell*, 97(7): 889-901.

Hu J, Castets F, Guevara JL, Van Eldik LJ. 1996. S100B stimulates inducible nitric oxide synthase activity, and mRNA levels in rat cortical astrocytes. *Journal of Biological Chemistry* 271: 2543-2547.

Hu J, Van Eldik LJ. 1999. Glial derived proteins activate cultured astrocytes and enhance β-amyloid-induced astrocyte activation. *Brain Research* 842: 46-54.

Huttunen HJ, Kuja-Panula J, Sorci G. 2000. Coregulation of neurite outgrowth and cell survival by amphoterin and S100 proteins through RAGE activation. *Journal of Biological Chemistry* 275: 40096–40105.

Joseph JA, Shukitt-Hale B, Denisova NA, Prior RL, Cao G, Martin A, Taglialatela G, Bickford PC. 1998. Long-term dietary strawberry, spinach, or vitamin E supplementation retards the onset of age-related neuronal signal-transduction and cognitive behavioral deficits. *Journal of Neuroscience* 18(19): 8047-8055.

Kilby PM, Van Eldik LJ, Roberts GCK. 1996. The solution structure of bovine S100B dimmer in the calcium-free state. *Structure* 1041-1052.

Kligman D, Marshak D. 1985. Purification and characterization of a neurite extension factor from bovine brain. *Proceedings of the National Academy of Sciences* 82: 7136-7410.

Kontush A, Mann U, Arlt S, Ujeyl A, Luhrs C, Muller-Thomsen T, Beisiegel, U. 2001. Influence of vitamin E and C supplementation on lipoprotein oxidation in patients with Alzheimer's disease. *Free Radical Biology & Medicine* 31(3): 345-354.

Kontush K, Schekatolina S. 2004. Vitamin E in neurodegenerative disorders: Alzheimer's disease. *Ann N Y Acad Sci* 1031:249-262.

Koppal T, Lam AG, Guo L, Van Eldik LJ. 2001. S100B proteins that lack one or both cysteine residues can induce inflammatory responses in astrocytes and microglia. *Neurochemistry International* 39(5-6): 401-407.

Landar A, Hall TL, Cornwall EH, Correia JJ, Drohat AC, Weber DJ, Zimmer DB. 1997. The role of cysteine residues in S100B dimerization and regulation of target protein activity. *Biochim Biophys Acta* 1343 (1): 117-129.

Lassmann H, Bancher C, Breitschopf H, Wegiel J, Bobinski M, Jellinger K, Wisniewski HM. 1995. Cell death in Alzheimer's disease evaluated by DNA fragmentation in situ. *Acta Neuropathol* 89(1): 35-41.

Leong SK, Ling EA. 1992. Amoeboid and ramified microglia: their interrelationship and response to brain injury. *Glia* 6(1): 39-47.

Li Y, Barger SW, Liu L, Mrak RE, Griffin WST. 2000. S100β induction of the proinflammatory cytokine interleukin-6 neurons. *Journal of Neurochemistry* 74: 143-150.

Liu Q, Xie F, Rolston R, Moreira PI, Nunomura A, Zhu X, Smith MA, Perry G. 2007. Prevention and treatment of Alzheimer disease and aging: antioxidants*. Mini Reviews in Medicinal Chemistry* 7(2): 171-180.

Lott IT, Head E. 2001. Down syndrome and Alzheimer's disease: a link between development and aging. *Mental Retardation and Developmental Disabilities Research Review 7*(3): 172-178.

Mariggio MA, Fulle S, Calissano P, Nicoletti I, Fano G. 1994. The brain protein S100ab induces apoptosis in PC12 cells. *Neuroscience* 60: 29-35.

Matsunaga, N, Anan I, Forsgren S, Nagai R, Rosenberg P, Horiuchi S, Ando Y, Suhr OB. 2002. Advanced glycation end products (AGE) and the receptor for AGE are present in gastrointestinal tract of familial amyloidotic polyneuropathy patients but do not induce NF-kappaB activation. *Acta Neuropathol (Berl), 104*(5), 441-470.

McGeer PL, Itagaki S, Tago H, McGeer EG. 1987. Reactive microglia in patients with senile dementia of the Alzheimer's type are positive for the histocompatibility glycoprotein HLA-DR. *Neuroscience Letters* 79: 195-200.

McGeer PL, McGeer EG. 2001. Inflammation, autotoxicity and Alzheimer's disease. *Neurobiology of Aging* 22: 799-809.

Mitchell JB, Lupica CR, Dunwiddie TV. 1993**.** Activity-dependent release of endogenous adenosine modulates synaptic responses in the rat hippocampus. *Journal of Neuroscience* 13: 3439-3447.

Moore BW. 1965. A soluble protein characteristic of the nervous system. *Biochemica Biophysica Research Communications, 19*, 739-744.

Muller CM, Akhavan AC, Bette M. 1993. Possible role of S-100 in glia-neuronal signaling involved in activity dependent plasticity in the developing mammalian cortex. *Journal of Chemistry and Neuroanatomy* 6:215-220.

Nakashima H, Ishihara T, Yokota O, Terada S, Trojanowski JQ, Lee VM, Kuroda S. 2004. Effects of α-tocopherol on an animal model of tauopathies. *Free Radical Biology & Medicine* 37(2): 176-186.

Nardin P, Tramontina F, Leite MC, Tramontine AC, Quincozes-Santos A, de Almeida LM, Battastini AM, Gottfried C, Goncalves CA 2007. S100B content and secretion decrease in astrocytes cultured in high-glucose medium. *Neurochemistry International* 50(5): 774-782.

Neeper M., Schmidt AM, Brett J, Yan SD, Wang F, Pan YC, Elliston K, Stern D, Shaw A. 1992. Cloning and expression of a cell surface receptor for advanced glycosylation end products of proteins. *Journal of Biological Chemistry, 267*(21), 4998-5004.

Parker TG, Marks A, Tsoporis JN. 1998. Induction of S100B in myocardium: an intrinsic inhibitor of cardiac hypertrophy. *Canadian Journal of Applied Physiology* 23(4): 377-389.

Paxinos G, Franklin K. 2001. The mouse brain in stereotaxic coordinates (2nd ed.) New York: Academic Press.

Perrone S, Longini M, Bellieni CV, Centini G, Kenanidis A, De Marco L, Petraglia F, Buonocore G. 2007. Early oxidative stress in amniotic fluid of pregnancies with Down syndrome. *Clinical Biochemistry* 40(3-4): 177-180.

Perry VH, Hume DA, Gordon S. 1985. Immunohistochemical localization of macrophages and microglia in the adult and developing mouse brain. *Neuroscience* 15(2): 312-326.

Petrova TV, Hu J, Van Eldik LJ. 2000. Modulation of glial activation by astrocytes-derived protein S100B: differential responses of astrocytes and microglia cultures. *Brain Research* 853: 74-80.

Portela LVC, Tort ABL, Schaf DV, Ribeiro L, Nora DB, Walz R, Rotta LN, Silva CT, Busnello JV, Kapczinski F, Goncalves CA, Souza DO 2002. The serum S100B concentration is age dependent. *Clinical Chemistry* 48(6): 950-952.

Praticò D. 2001. Vitamin E: murine studies versus clinical trials. *Ital. Heart J.* 2:878-881.

Richter-Landsber C, Heinrich M. 1995. S-100 immunoreactivity in rat brain glial cultures is associated with both astrocytes and oligodendrocytes. *Journal of Neuroscience Research* 42(5): 657-665.

Rogers J, Luber-Narod J, Styren SD, Civin WH. 1988. Expression of immune system-associated antigens by cells of the human central nervous system: relationship to the pathology of Alzheimer's disease. *Neurobiology of Aging* 9(4): 339-349.

Rogers J, Strohmeyer R, Kovelowski CJ, Li R. 2002. Microglia and inflammatory mechanisms in the clearance of amyloid beta peptide. *Glia* 40(2): 260-269.

Rothermundt M, Peters M, Prehn JH, Arolt V. 2003. S100B in brain damage and neurodegeneration. *Microscopy Research Technology* 60(6): 614-632.

Sano M, Ernesto C, Thomas RG, Klauber MR, Schafer K, Grundman M, Woodbury P, Growdon J, Cotman CW, Pfeiffer E, Schneider LS, Thal LJ. 1997. A controlled trial of selegiline, α-tocopherol, or both as treatment for Alzheimer's disease. The Alzheimer's Disease Cooperative Study. *New England Journal of Medicine* 336: 1216-1222.

Schmidt AM, Yan SD, Yan SF, Stern DM. 2000. The biology of the receptor for advanced glycation end products and its ligands. *Biochimica et Biophysica Acta* 1498(2-3): 99-111.

Schonheit B, Zarski, R, Ohm TG. 2004. Spatial and temporal relationships between plaques and tangles in Alzheimer-pathology. *Neurobiology of Aging* 25: 697-711.

Scotto C, Mely Y, Ohshima H, Garin J, Cochet C, Chambaz E, Baudier J. 1998. Cysteine oxidation in the mitogenic S100B protein leads to changes in phosphorylation by catalytic CKII-alpha subunit. *Journal of Biological Chemistry* 273: 3901-3908.

Selinfreund RH, Barger SW, Pledger WJ, Van Eldik LJ. 1991. Neurotrophic protein S100 beta stimulates glial cell proliferation. *Proceedings of the National Academy of Sciences USA* 88(9): 3554-3558.

Sen J, Belli A. 2007. S100B in neuropathologic states: the CRP of the brain? *Journal of Neuroscience Research* 85(7): 1373-1380.

Shapiro, LA. 2003. The Role of S-100B in CNS Development, Maintenance and Pathology. A dissertation from Stony Brook University.

Shapiro LA, Marks A, Whitaker-Azmitia PM. 2004. Increased clusterin expression in old but not young S100B transgenic mice: evidence of neuropathological aging in a model of Down Sydrome. *Brain Research* 1010(1-2): 17-21.

Shapiro LA, Whitaker-Azmitia PM. 2004. Expression levels of cytoskeletal proteins indicate pathological aging of S100B transgenic mice: an immunohistochemical study of MAP-2, drebrin and GAP-43. *Brain Research* 1019(1-2): 39-46.

Singh N, Pillay V, Choonara YE. 2007 Advances in the treatment of Parkinson's disease. *Progress in Neurobiology* 81(1): 29-44.

Smith MA, Rottkamp CA, Nunomura A, Raina AK, Perry G. 2000. Oxidative stress in Alzheimer's disease. *Biochim Biophys Acta* 1502: 139-144.

Smith SP, Shaw GS. 1998a. A change-in-hand mechanism for S100 signaling. *Biochemistry and Cell Biology* 76(2-3): 324-333.

Smith SP, Shaw GS. 1998b. A novel calcium-sensitive switch revealed by the structure of human S100B in the calcium-bound form. *Structure* 6(2): 211-222.

Spector R. 1977. Vitamin homeostasis in the central nervous system. *New England Journal of Medicine* 296: 1393-1398.

Stolzing A, Widmer R, Jung T, Voss P, Grune T. 2006. Tocopherol-mediated modulation of age-related changes in microglial cells: turnover of extracellular oxidized protein material. *Free Radical Biology & Medicine* 40(12): 2126-35.

Streit WJ, 2004. Microglia and Alzheimer's Disease Pathogenesis. Journal of Neuroscience Review 77(1): 1-8.

Streit WJ, Graeber MB, Kreutzberg, GW. 1988. Functional plasticity of microglia: A review. *Glia*, 1: 301-307.

Streit WJ, Mrak RE, Griffin WS. 2004. Microglia and neuroinflammation: a pathological perspective. *Journal of Neuroinflammation* 1(1): 1-4.

Streit WJ, Sammons NW, Kuhns AJ, Sparks DL. 2004. Dystrophic microglia in the aging human brain. *Glia* 45(2): 208-212.

Streit WJ, Walter SA, Pennell NA. 1999. Reactive microgliosis. *Progress in Neurobiology*, 57(6): 563-581.

Sung S, Yao Y, Uryn K, Yang H, Lee VM, Trojanowski JQ, Practico D. 2003. Early vitamin E supplementation in young but not aged mice reduces Aβ levels and amyloid deposition in a transgenic model of Alzheimer's disease. *FASEB* 18(2):323-5

Thiel R, Fowkes SW. 2005 Can cognitive deterioration associated with Down syndrome be reduced? *Medical Hypotheses* 64(3): 524-532.

Tiu SC, Chan WY, Heizmann CW, Schafer BW, Shu SY, Yew DT. Differential expression of S100B and S100a6 in the human fetal and aged cerebral cortex. *Developmental Brain Research* 119: 119-159.

Tramontina F, Leite MC, Goncalves D, Tramontina AC, Souza DF, Frizzo JK, Nardin P, Gottfried C, Wofchuk ST, Goncalves CA. 2006. High glutamate decreases S100B secretion by a mechanism dependent on the glutamate transporter. *Neurochemistry Research* 6: 815-820.

Van Eldik LJ, Staecker JL, Winningham-Major F. 1988. Synthesis and expression of a gene coding for the calcium-modulated protein S100 beta and designed for cassette-based, site-directed mutagenesis. *Journal of Biological Chemistry* 263(16): 7830-7837.

Wang JY, Wen LL, Huang YN, Chen YT, Ku MC. 2006. Dual effects of antioxidants in neurodegeneration: direct neuroprotection against oxidative stress and indirect protection via suppression of glia-mediated inflammation. Current Pharmaceutical Design 12(27): 3521-3533.

Whitaker-Azmitia PM. Azmitia EC. 1989. Stimulation of astroglial serotonin receptors produces culture media which regulates growth of serotonergic neurons. *Brain Research* 497(1): 80-85.

Whitaker-Azmitia PM, Murphy R, Azmitia EC. 1990. Stimulation of astroglial 5-HT1A receptors releases the serotonergic growth factor, protein S-100, and alters astroglial morphology, *Brain Research* 528(1): 155-158.

Winningham-Major F, Staecker JL, Barger SW, Coats S, Van Eldik LJ. 1989. Neurite extension and neuronal survival activities of recombinant S100 beta proteins that differ in the content and position of cysteine residues. *The Journal of Cell Biology* 109 (6 pt 1): 3063-71.

Winocur G, Roder J, Lobaugh N. 2001. Learning and memory in S100-beta transgenic mice: an analysis of impaired and preserved function. *Neurobiology of Learning and Memory* 75(2): 230-243.

Yan W, Wilson CC, Haring JH. 1997. 5-HT1a receptors mediate the neurotrophic effect of serotonin on developing dentate granule cells. *Brain Research: Developmental Brain Research* 98: 185-190.

Zhukova L, Zhukov I, Bal W, Wyslouch-Cieszynska A. 2004. Redox modifications of the C-terminal cysteine residue cause structural changes in S100A1 and S100B proteins. *Biochim Biophys Acta* 1724(1-3): 191-201.

Zimmer DB, Cornwall EH, Landar A, Song W. 1995. The S100 protein family: history, function, and expression. *Brain Research Bulletin* 37(4):417-429.

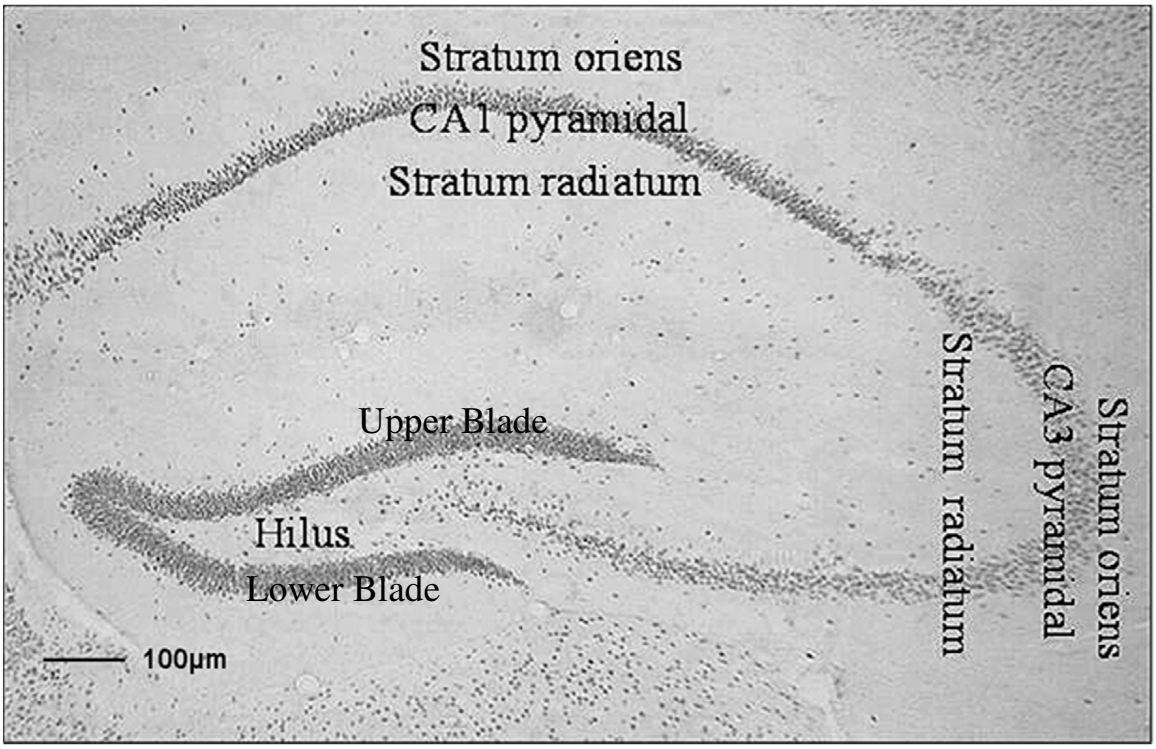

Figure 1. Representative photomicrograph of RAGE immunoreactivity of regions of interest used in all analyses (Experiment 1, 2a, 2b) (40X magnification).

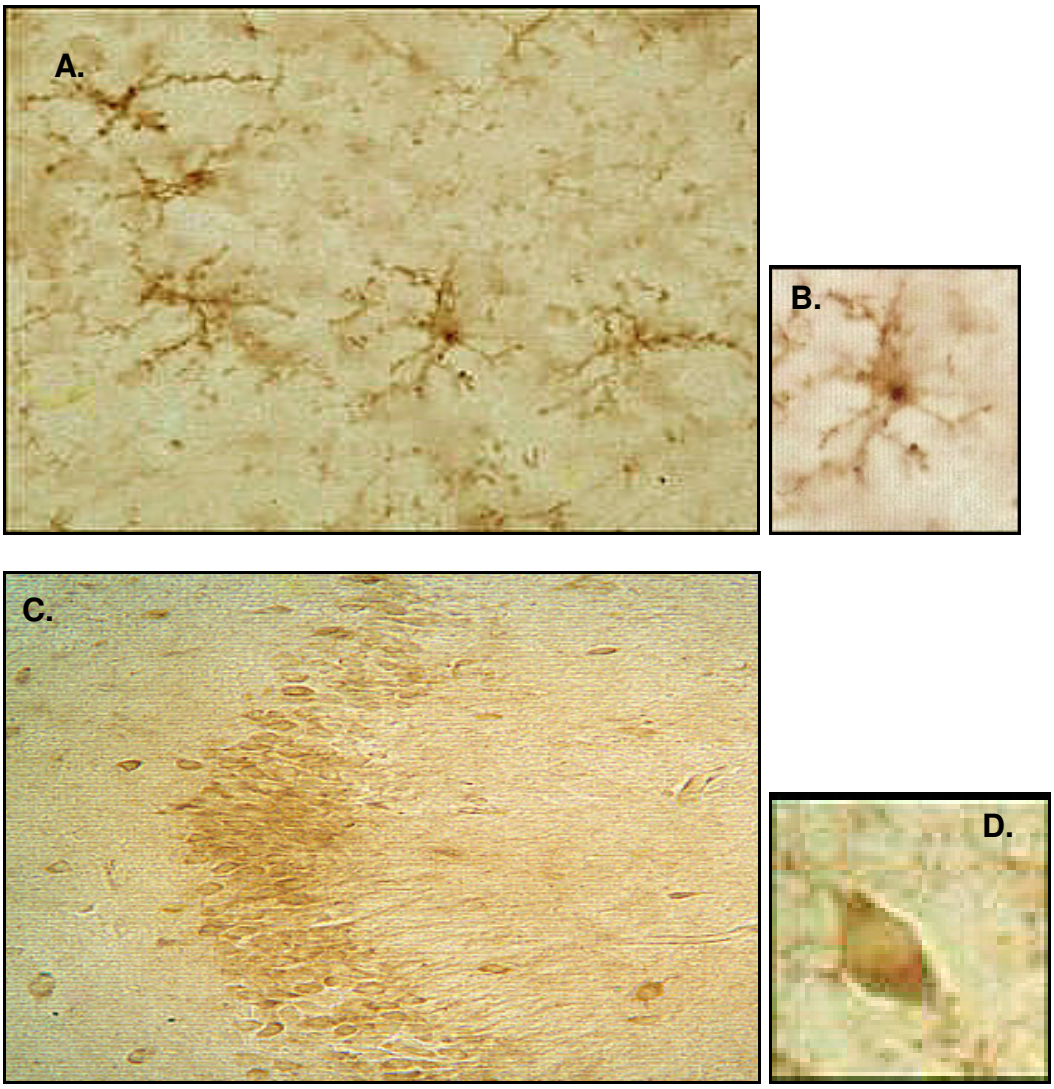

Figure 2. Representative photomicrographs of F4/80-postive microglial cells in the resting (A, B) and activated morphology (C, D). Resting cells bear a ramified morphology whereas activated cells appear phagocytic after retracting their processes to bear an ameboid shape.

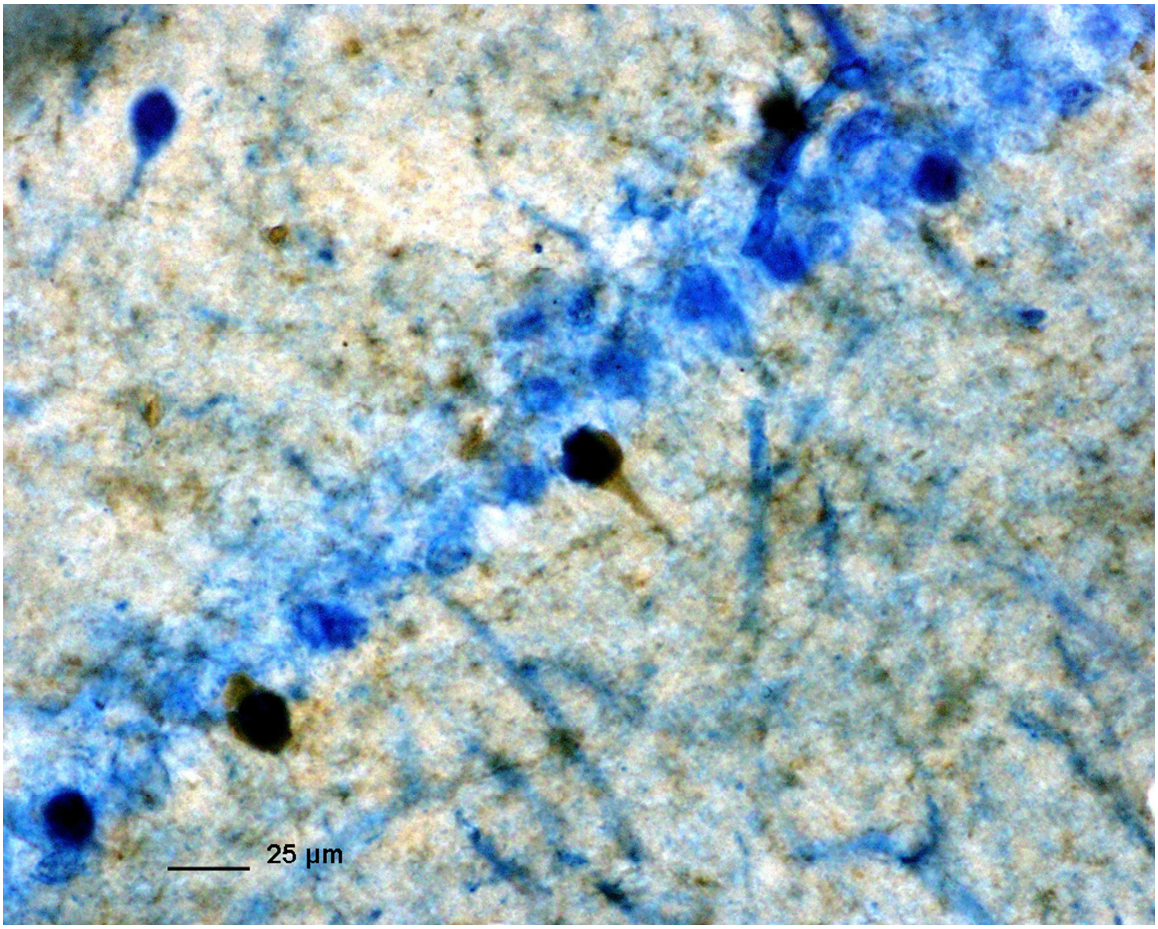

Figure 3. RAGE (blue) and microglia (brown) co-labeling in hippocampal CA3 of S100B control diet mice (400X). Majority of RAGE co-labeling occurred with activated cells in the pyramidal region as opposed to with resting cells in stratum oriens and radiatum.

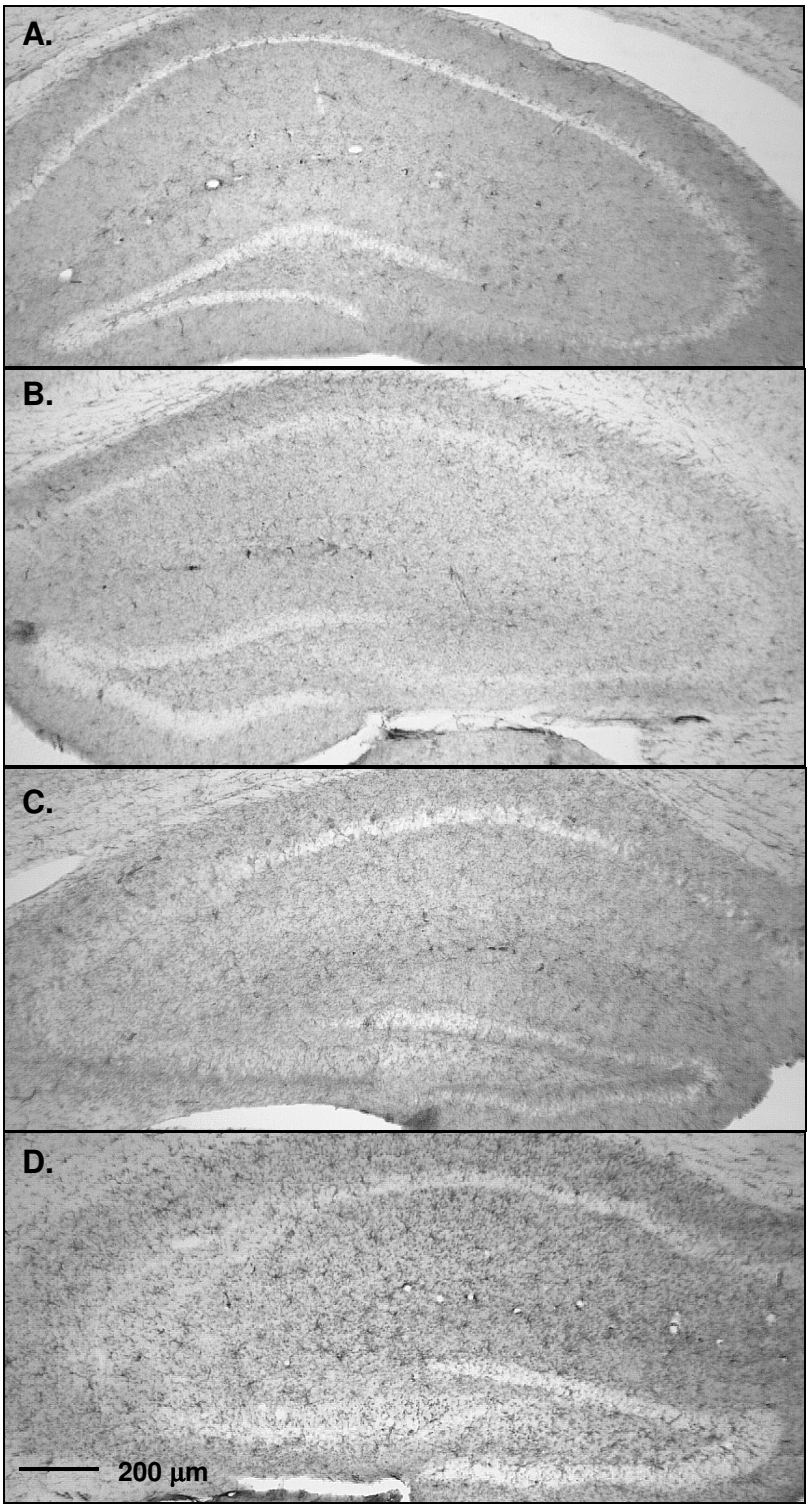

Figure 4. Representative photomicrographs of F4/80 microglial reactivity in the hippocampus of CD1 control animals at 1 month (A), 3 months (B), 6 months (C) and 12 months (D) of age (40X). Average immunodensity increases with age although the majority of cells remain in the ramified and resting morphology.

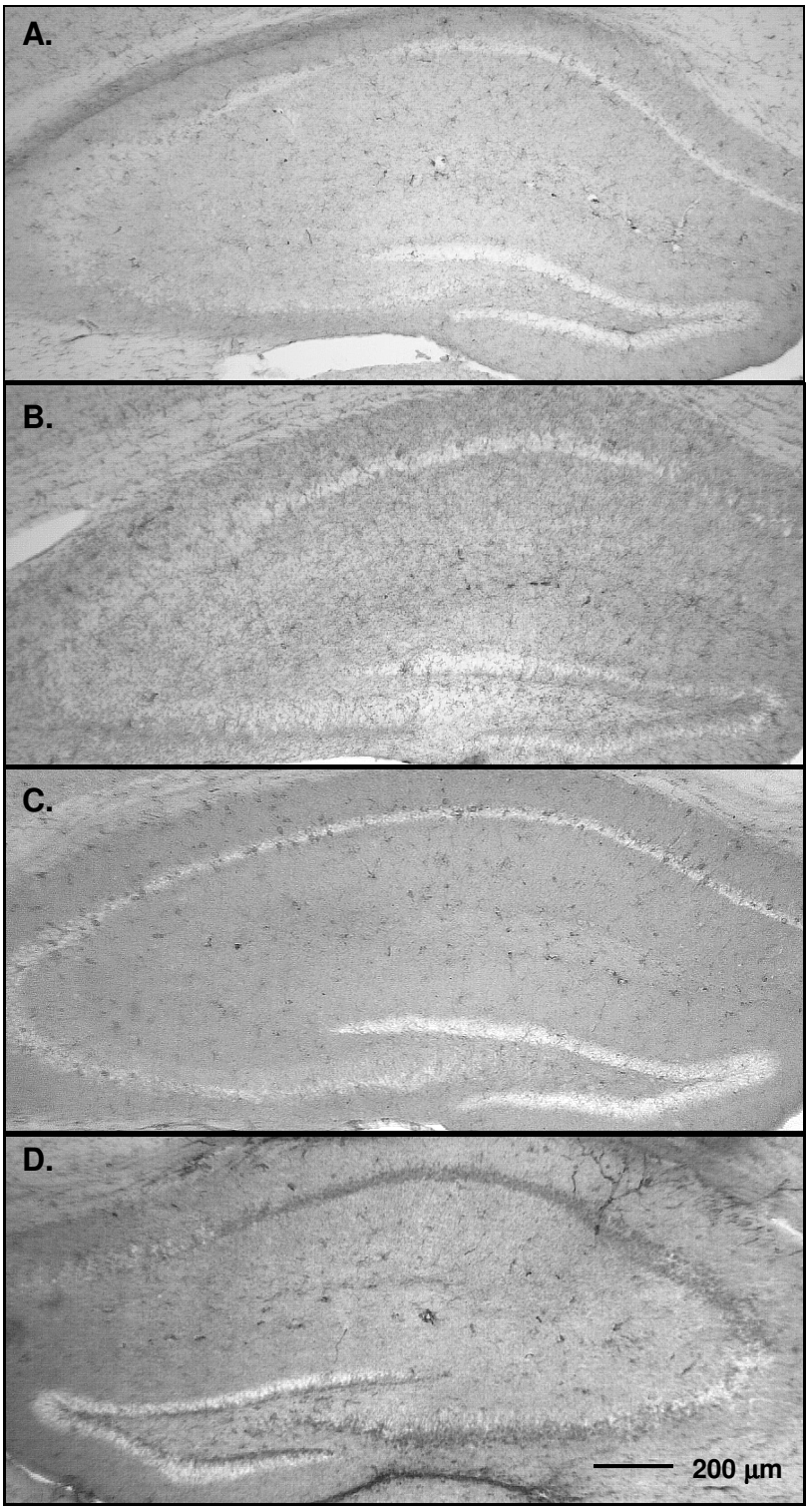

Figure 5. Representative photomicrographs of F4/80 microglial reactivity in the hippocampus of S100B-overexpressing animals at 1 month (A), 3 months (B), 6 months (C) and 12 months (D) of age (40X). Average immunodensity increases with age with a morphology progression from a ramified and resting state to an ameboid and activiated morphology.

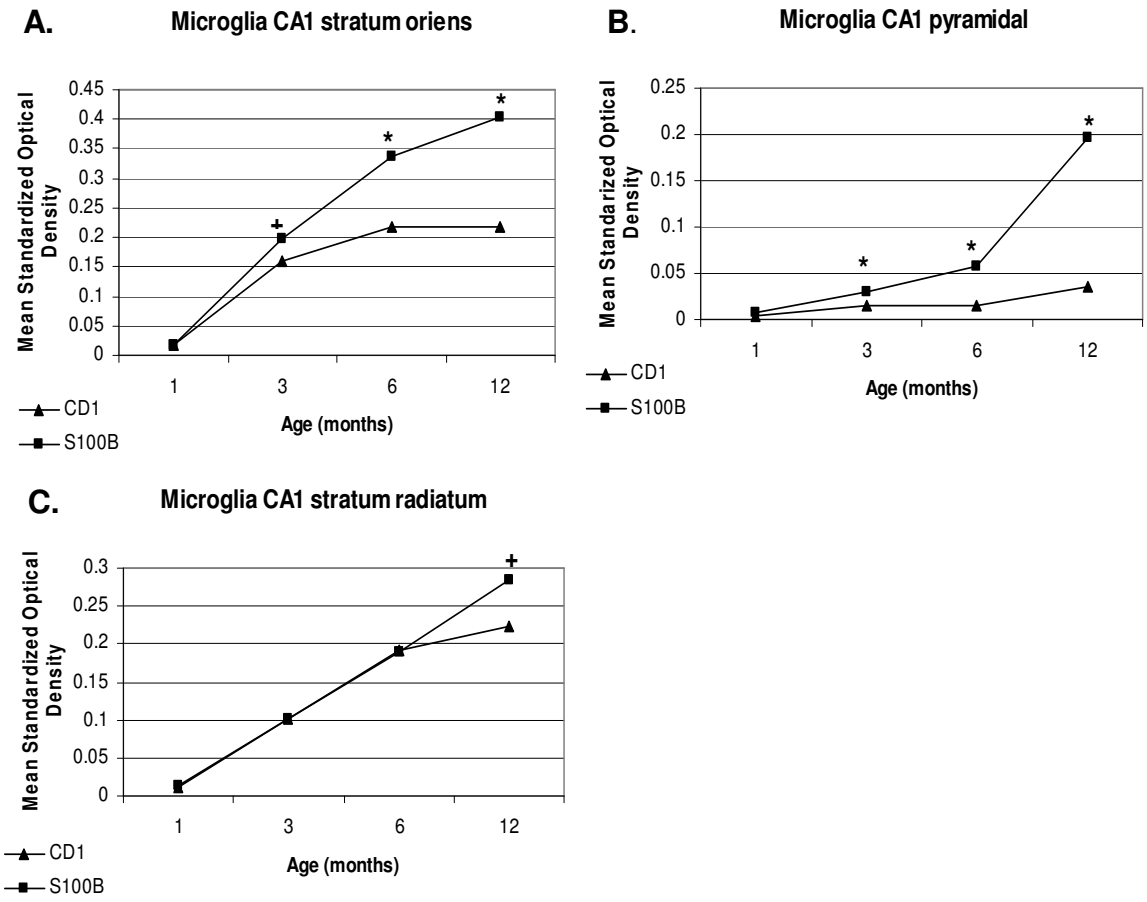

Figure 6. Main Effect of Strain on average F4/80 microglial immunodensity in CA1 stratum oriens (A), pyramidal (B), and stratum radiatum (C) at 1, 3, 6 and 12 months of age. S100B over-expressing mice had on average greater immunoreactivity than CD1 control animals, $^{*}p = 0.00$; $+ p < 0.05$.

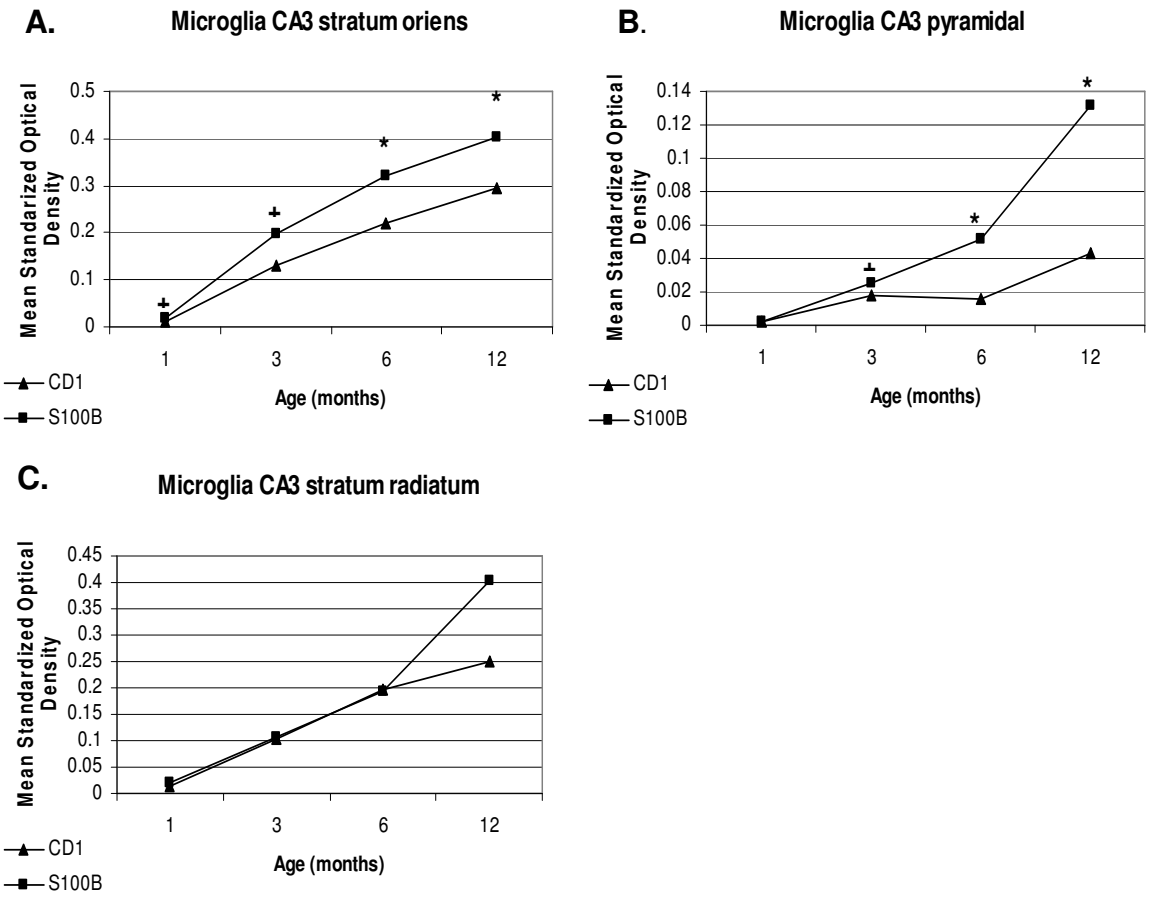

Figure 7. Main Effect of Strain on average F4/80 microglial immunodensity in CA3 stratum oriens (A), pyramidal (B), and stratum radiatum (C) at 1, 3, 6 and 12 months of age. S100B over-expressing mice had significantly greater average immunoreactivity than CD1 control animals, $*p = 0.00$; $+ p < 0.05$.

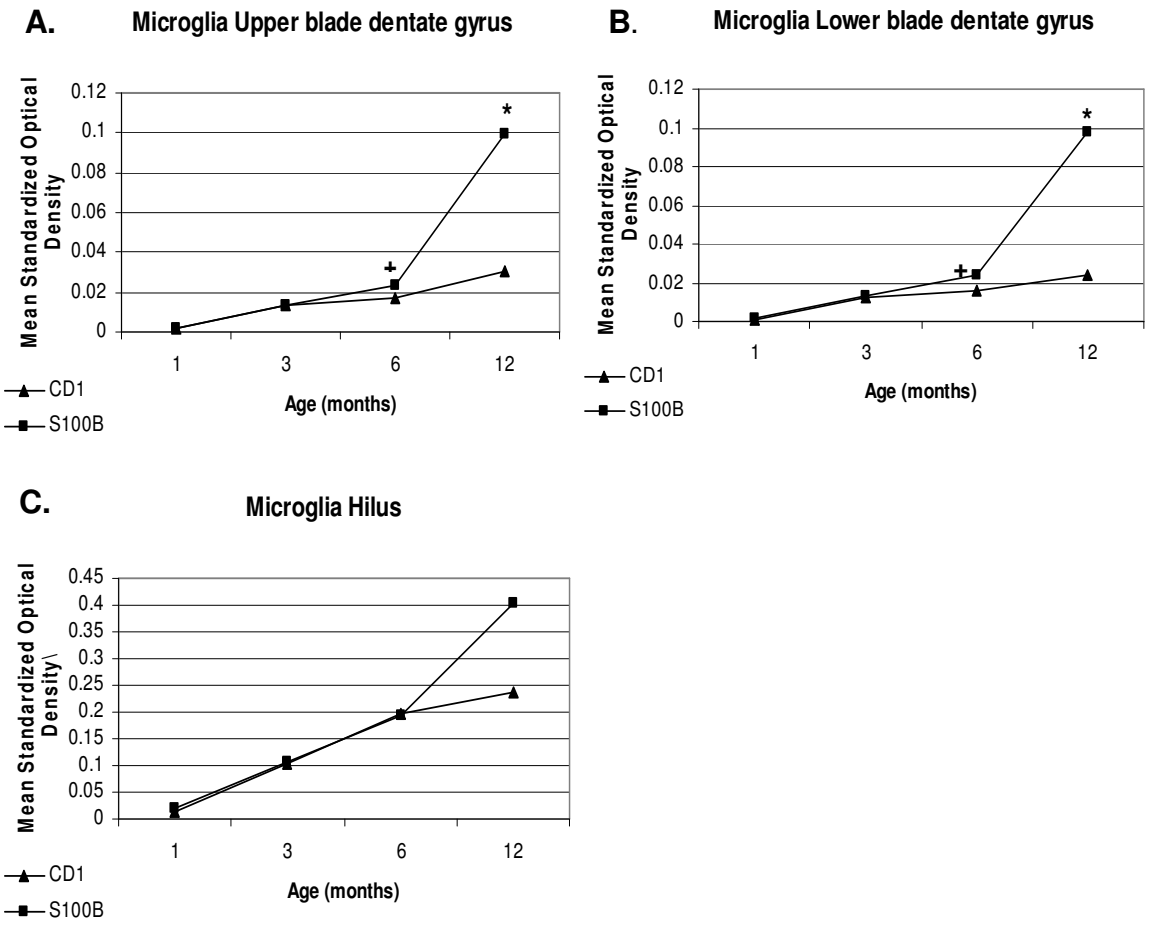

Figure 8. Main Effect of Strain on average F4/80 microglial immunodensity in dentate gyrus upper blade (A), lower blade (B), and hilus (C) at 1, 3, 6 and 12 months of age. S100B over-expressing mice had significantly greater average immunoreactivity than CD1 control animals, $*p = 0.00$; $+ p < 0.05$.

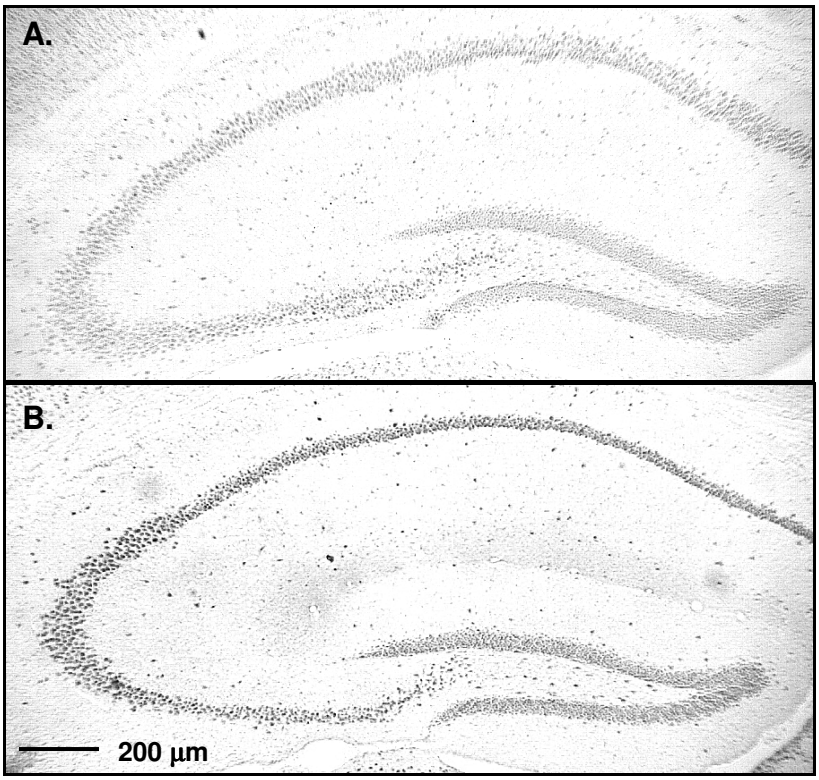

Figure 9. Representative photomicrograph of RAGE immunopositive cells in the hippocampus of CD1 control (A) and S100B-overexpressing mice (B) at six months of age (40X).

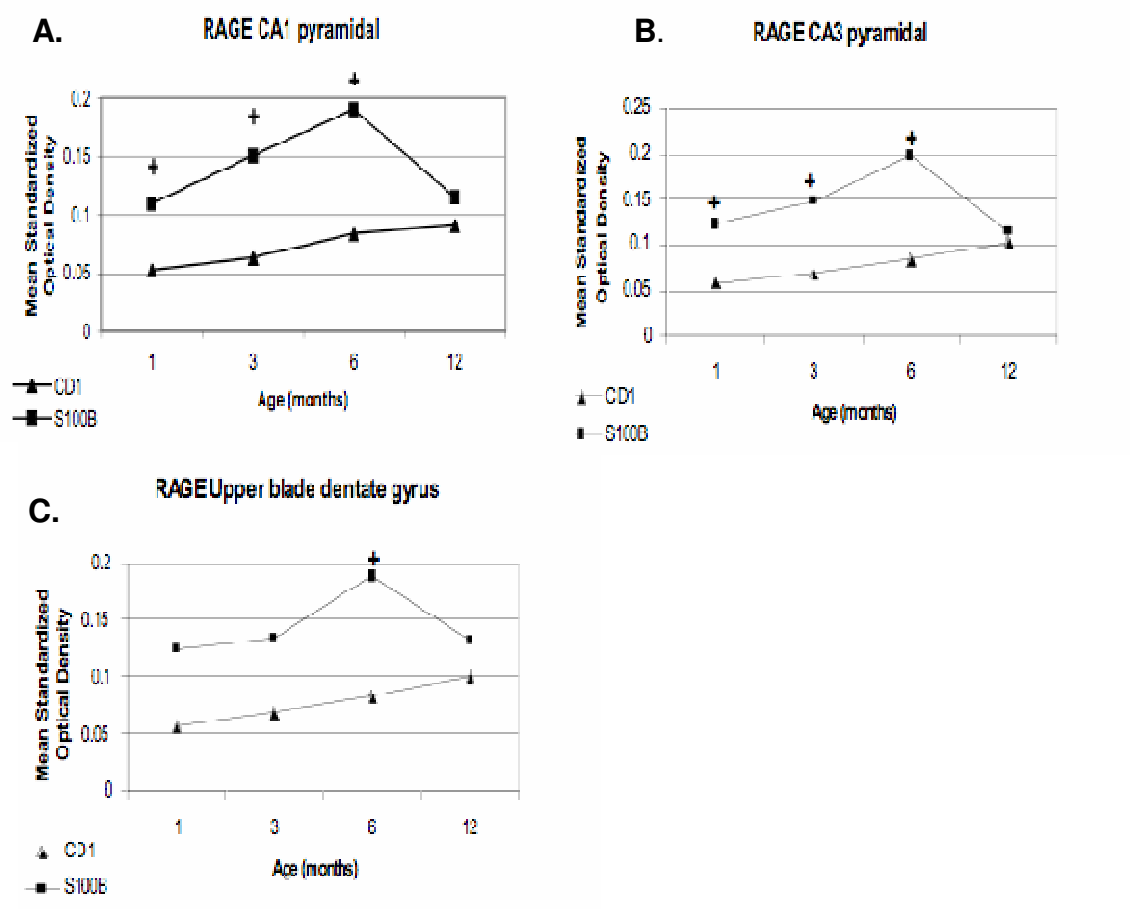

Figure 10. Main Effect of Strain on average RAGE expression in CA1 pyramidal (A), CA3 pyramidal (B), and upper blade of the dentate gyrus (C) at 1, 3, 6 and 12 months of age. S100B over-expressing mice had significantly greater average immunoreactivity than CD1 control animals, + $p < 0.05$.

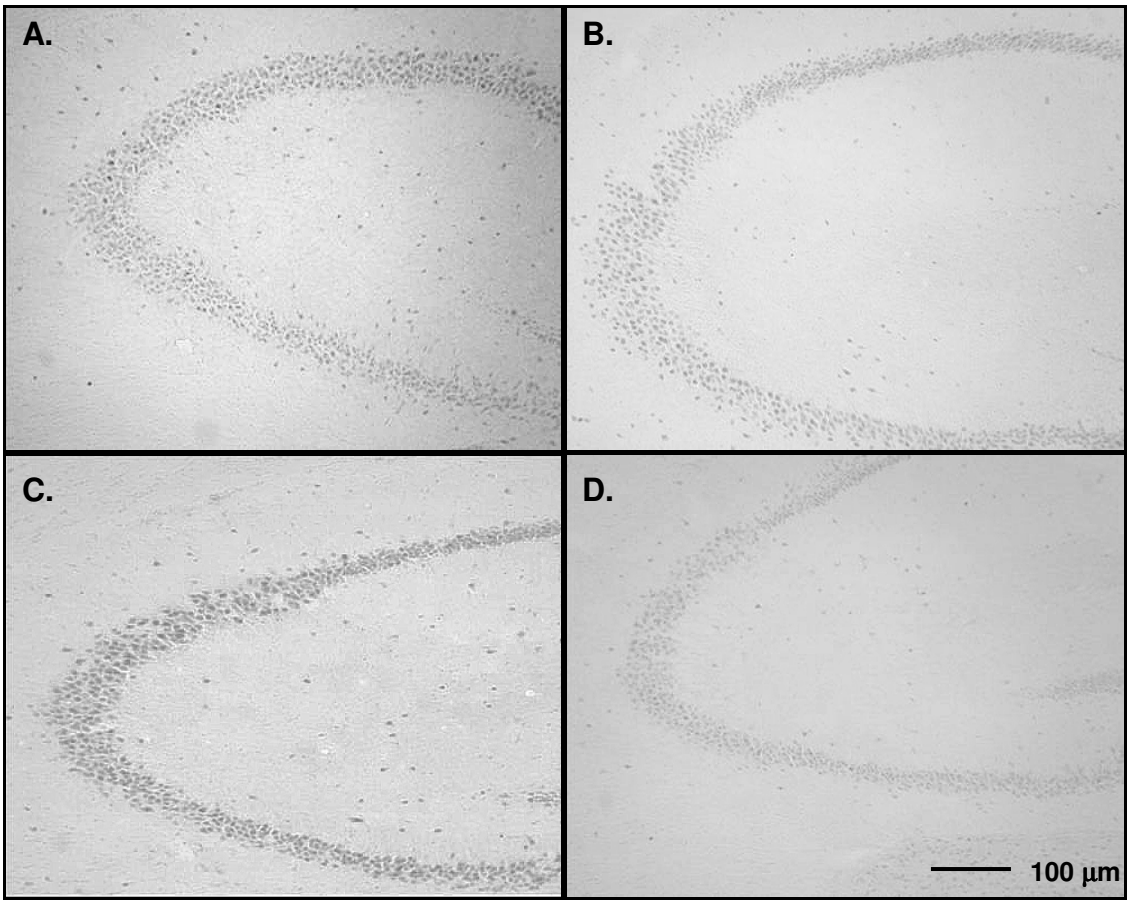

Figure 11. Representative photomicrographs of age-associated increases of RAGE immunopositive cells in hippocampal CA3 of CD1 control animals at 6 (A) and 12 (B) months and S100B overexpressing animals at 6 (C) and 12 (D) months of age (100X). S100B animals have significantly greater reactivity than CD1 animals at 1, 3 and 6 months. By 12 months of age, CD1 animals display greater reactivity than S100B-overexpressing mice.

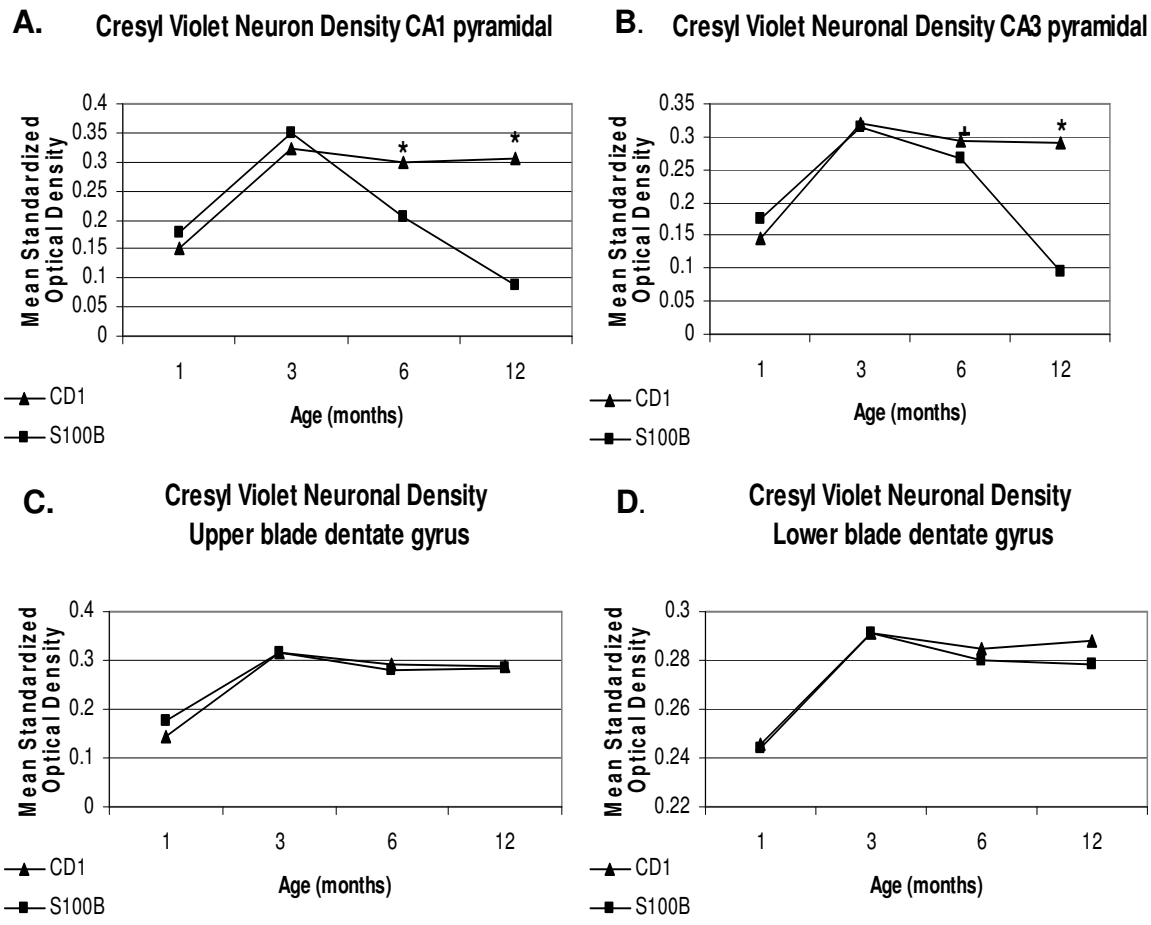

Figure 12. Main Effect of Strain on average cresyl violet neuronal density in CA1 pyramidal (A), CA3 pyramidal (B), upper blade (C) and lower blade of the dentate gyrus (D) at 1, 3, 6 and 12 months of age. CD1 control animals had significantly greater average immunoreactivity than S100B-overexpressing animals, *p = 0.00; + $p < 0.05$.

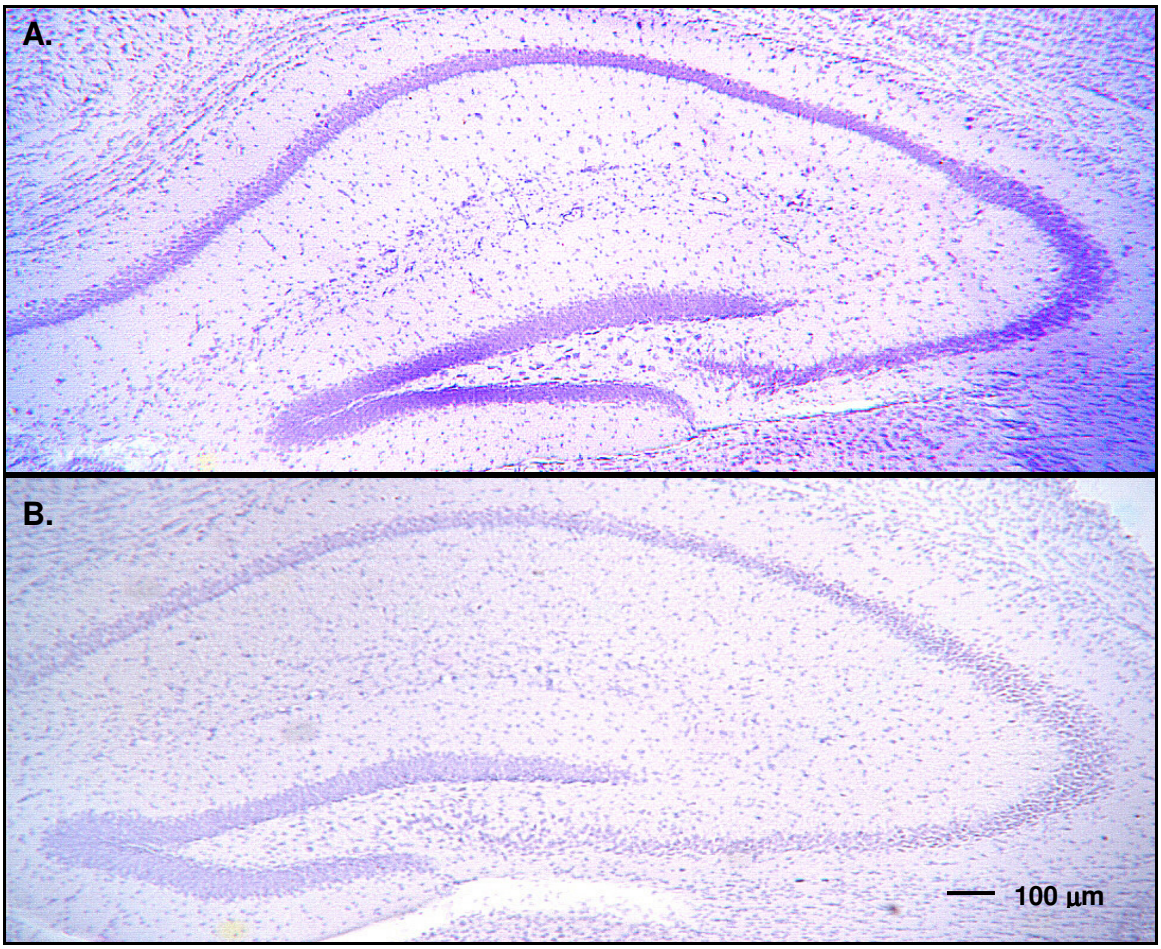

Figure 13. Representative photomicrographs of cresyl violet neuronal cell bodies in the hippocampus of CD1 (A) and S100B-overexpressing (B) mice at 12 months of age (40X). S100B-overexpressing animals have significantly less hippocampus neuronal density than CD1 control animals at one year of age.

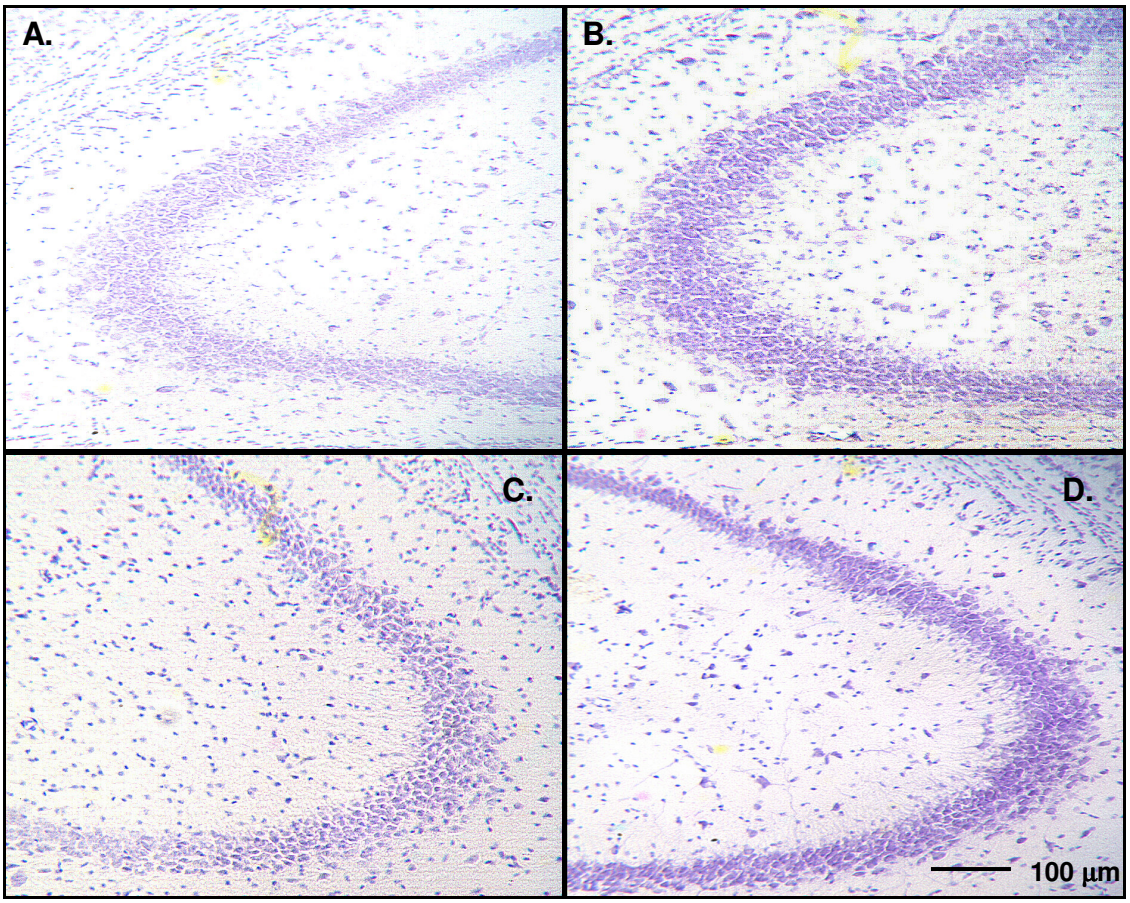

Figure 14. Representative photomicrographs of cresyl violet neuronal cell bodies in hippocampal CA3 of CD1 control animals at 1 (A), 3 (B), 6 (C) and 12 (D) months of age (100X). Immunodensity significantly increases from 1-3 months of age and remains consistent until 12 months.

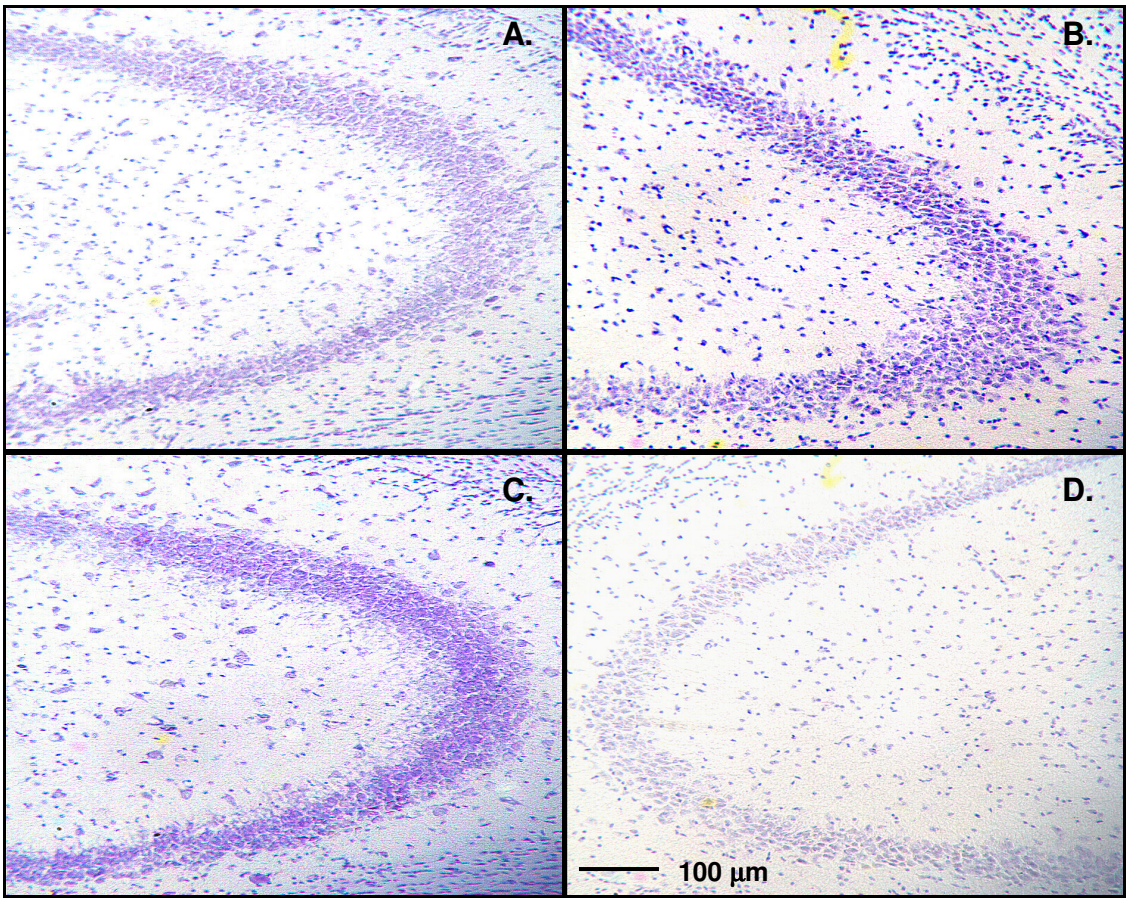

Figure 15. Representative photomicrographs of cresyl violet neuronal cell bodies in hippocampal CA3 of S100B-overexpressing animals at 1 (A), 3 (B), 6 (C) and 12 (D) months of age (100X). Immunodensity significantly increases from 1-3 months of age and significantly declines between 6 and 12 months of age.

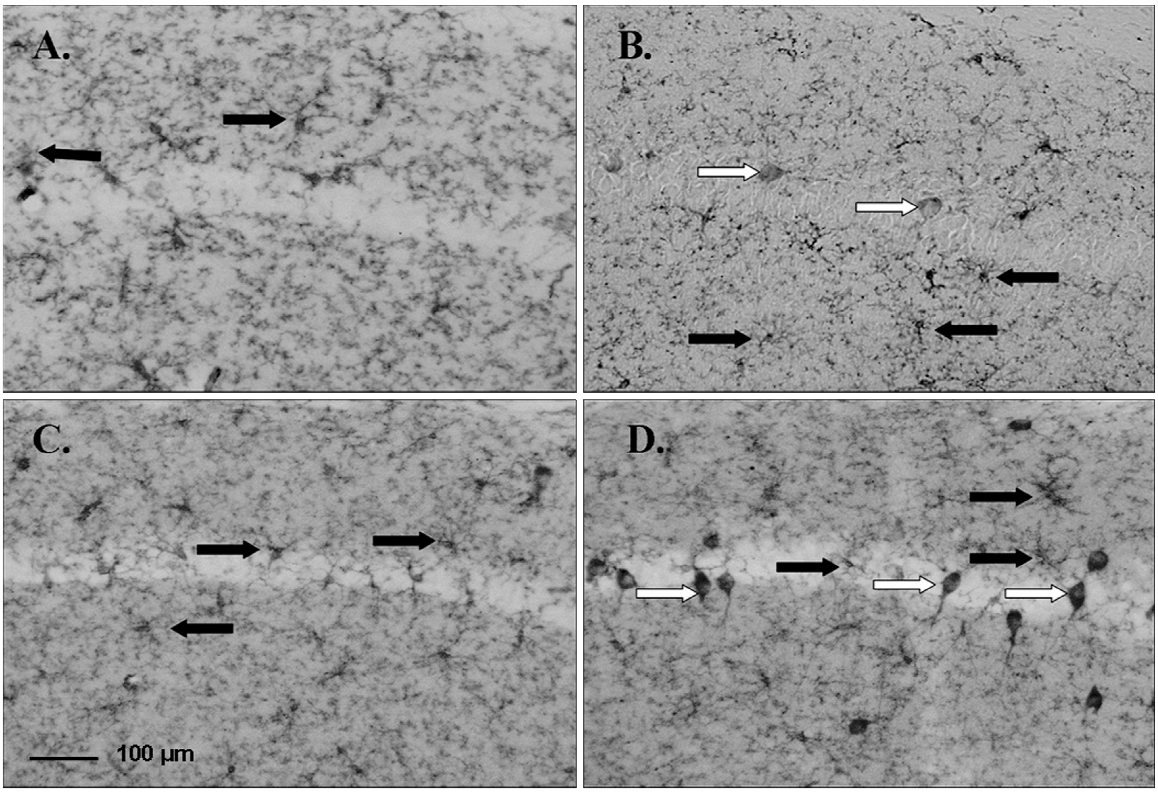

Figure 16. F4/80 immunoreactivity of resting (solid arrow) and activated (white arrow) microglia in CD1 control diet (A), Vitamin E diet (B), and S100B control diet (C), Vitamin E diet (D) animals in CA1 pyramidal, stratum oriens, and stratum radiatum (200X).

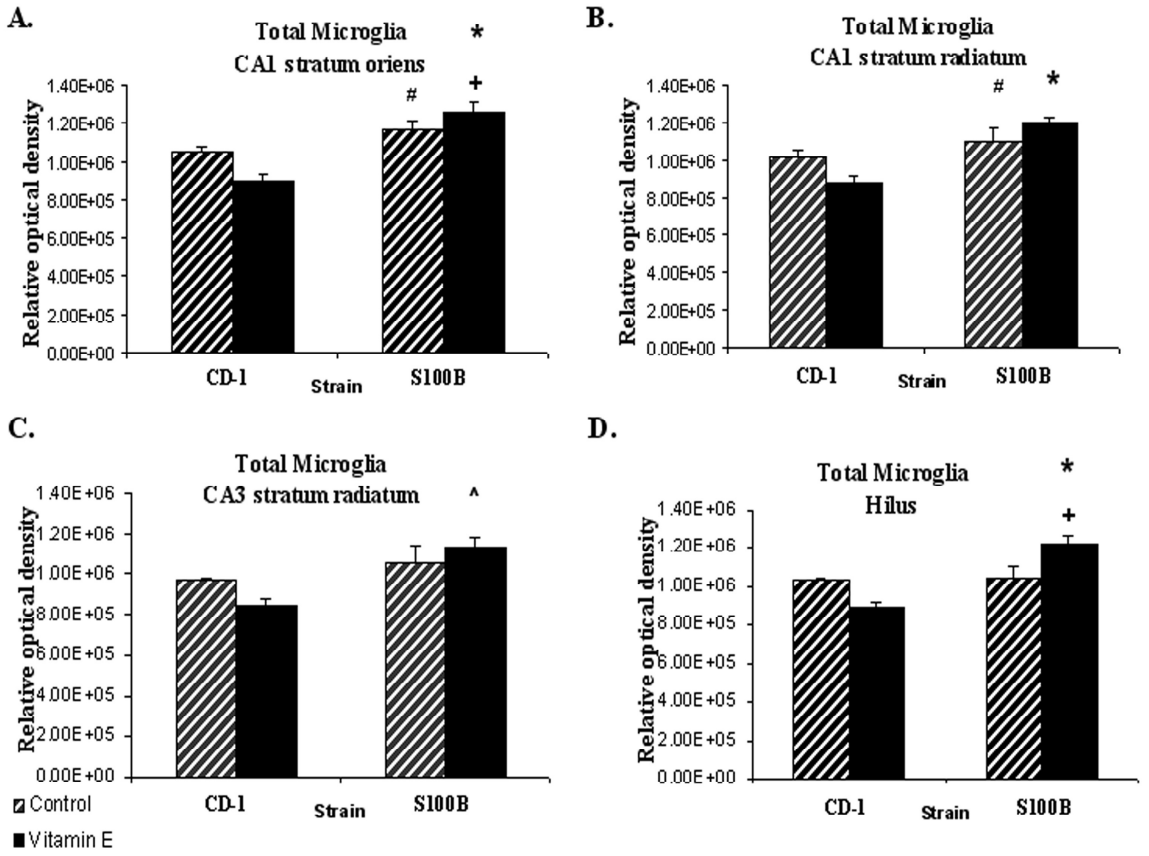

Figure 17. Average F4/80 microglial immunodensity in CA1 stratum oriens (A), CA1 stratum radiatum (B), CA3 stratum radiatum (C) and hilus (D). S100B Vitamin E had greater immunoreactivity than CD1 Vitamin E (A, B and D), * $p <$ 0.005, + $p < 0.01$, and CD1 control diet animals (C),^ $p < 0.05$. S100B control diet had greater reactivity than CD1 vitamin E mice (A and B), # $p < 0.05$.

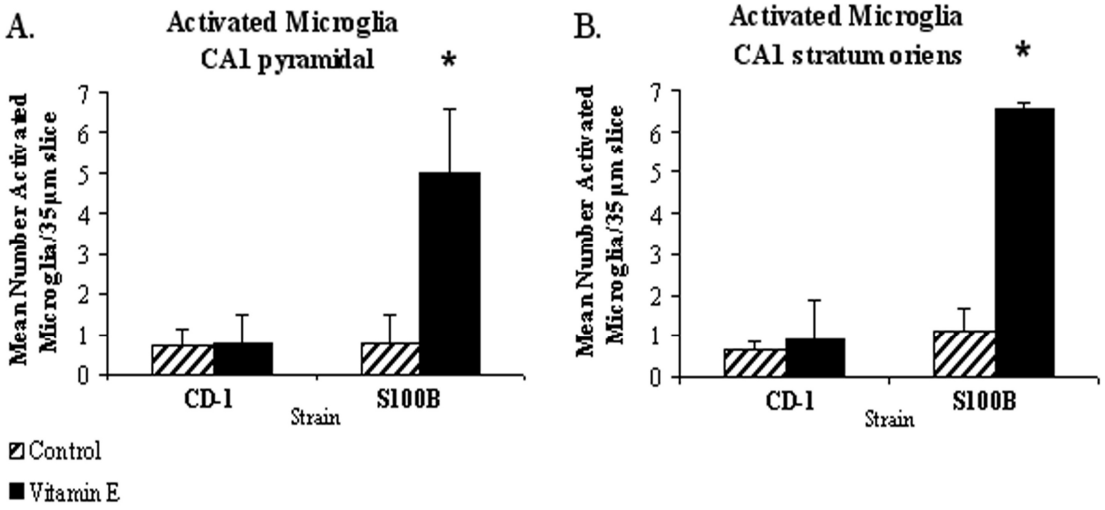

Figure 18. Average number of F4/80 activated microglia in CA1 pyramidal (A) and stratum oriens (B). S100B vitamin E mice expressed greatest number of activated cells * $p < 0.02$.

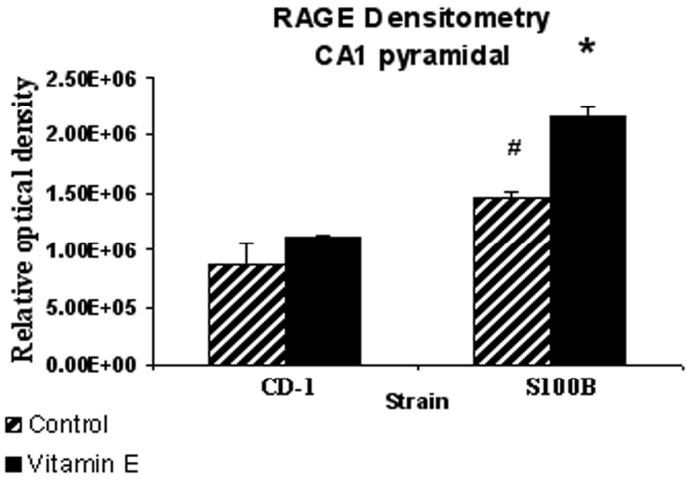

Figure 19. RAGE immunodensity in hippocampal CA1 pyramidal cells. S100B vitamin E had greater RAGE expression than S100B control diet or CD1 animals on either diet, $*p < 0.002$. S100B control diet had more reactivity than CD1 control diet animals, $\# p < 0.015$.

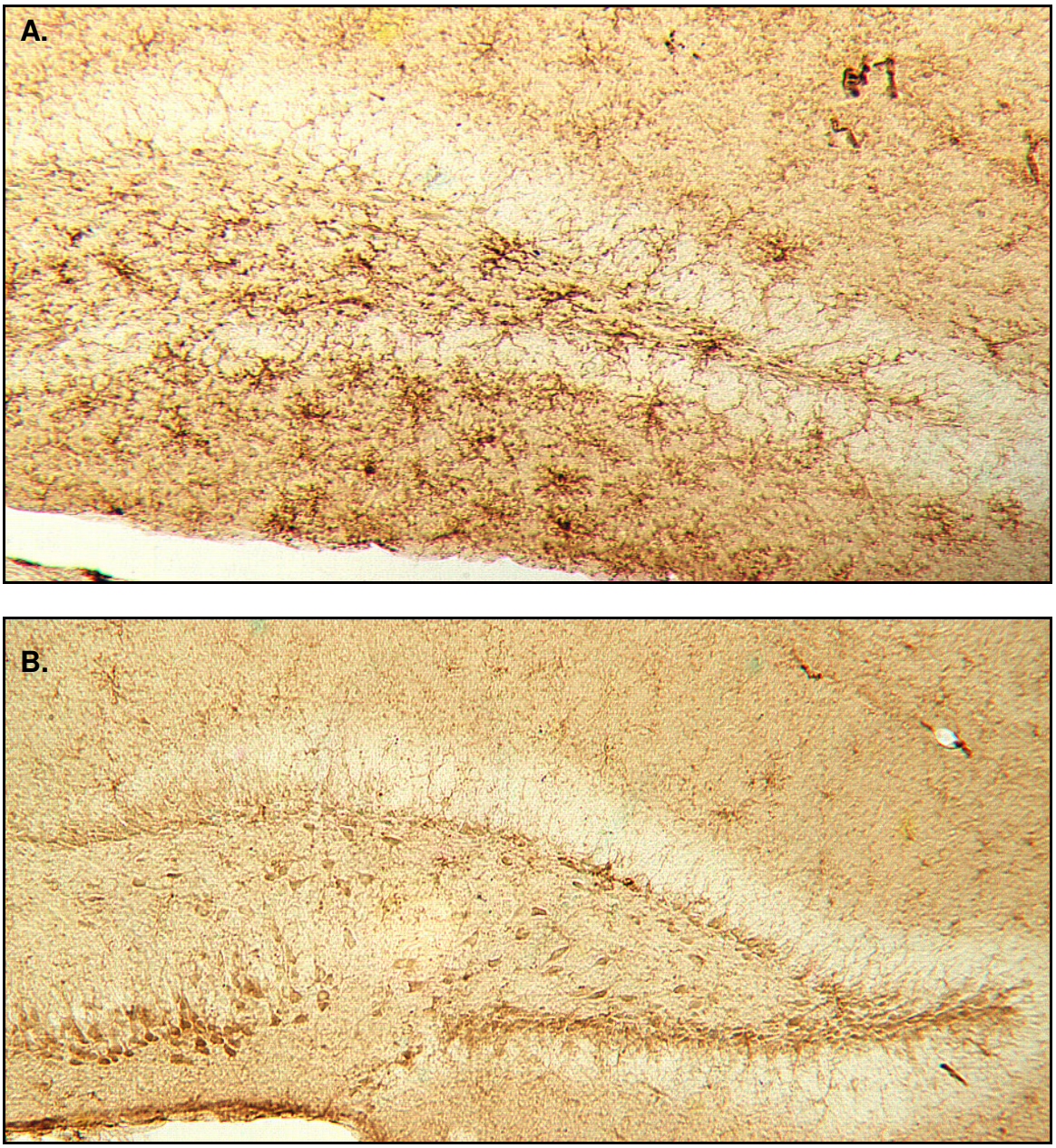

Figure 20. Representative photomicrograhs of F4/80 immunopositive microglial cells in the dentate gyrus of CD1 control diet (A) and S100B-overexpressing Vitamin E diet (B) mice. CD1 animals appear to have the majority of the microglial cells in the resting state as opposed to the S100B mice express the greatest pattern of reactivity in the activated morphology.

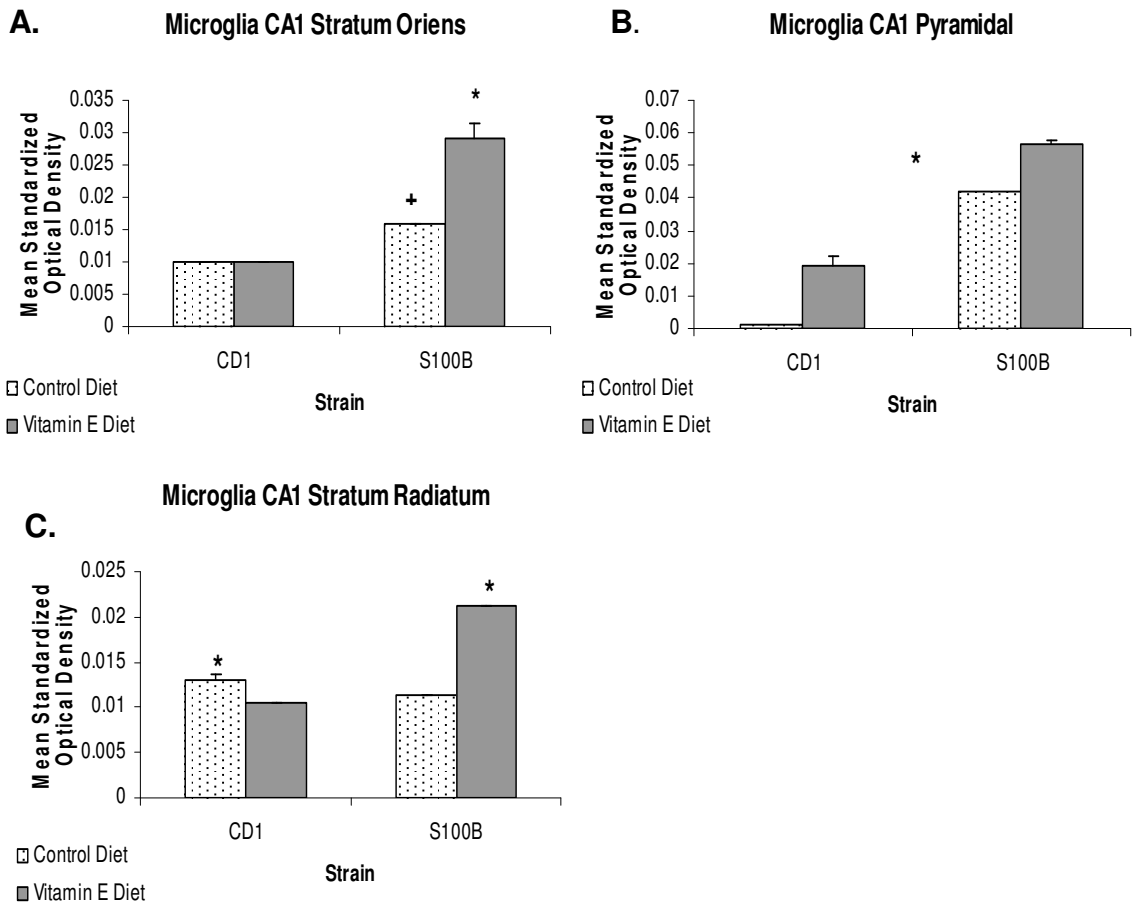

Figure 21. Average F4/80 microglial immunodensity in CA1 stratum oriens (A), pyramidal (B), and stratum radiatum (C). S100B Vitamin E animals had greater immunoreactivity (A,B,C) than all other groups, $*p < 0.01$. In CA1 stratum oriens, S100B control diet animals had greater reactivity than CD1 animals on either diet (A), $p < 0.05$. Within CA1 pyramidal (B), all groups were significantly different from each other, $*p < 0.01$. In CA1 stratum radiatum, CD1 control diet animals had significantly greater reactivity than CD1 Vitamin E and S100B control diet animals (C), $*p < 0.01$.

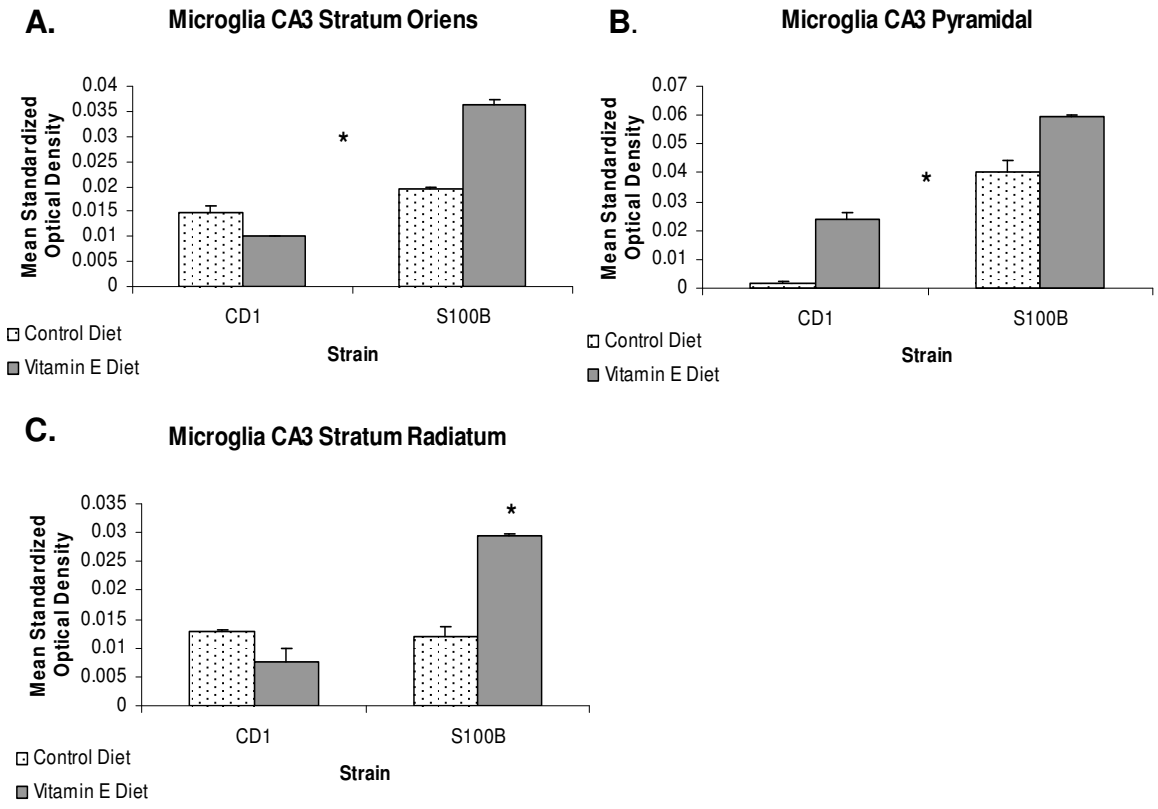

Figure 22. Average F4/80 microglial immunodensity in CA3 stratum oriens (A), pyramidal (B), and stratum radiatum (C). S100B Vitamin E animals had greater immunoreactivity (A,B,C) than all other groups, $*p < 0.01$. Within CA3 stratum oriens (A) and pyramidal (B), all groups were significantly different from each other, $*p < 0.01$.

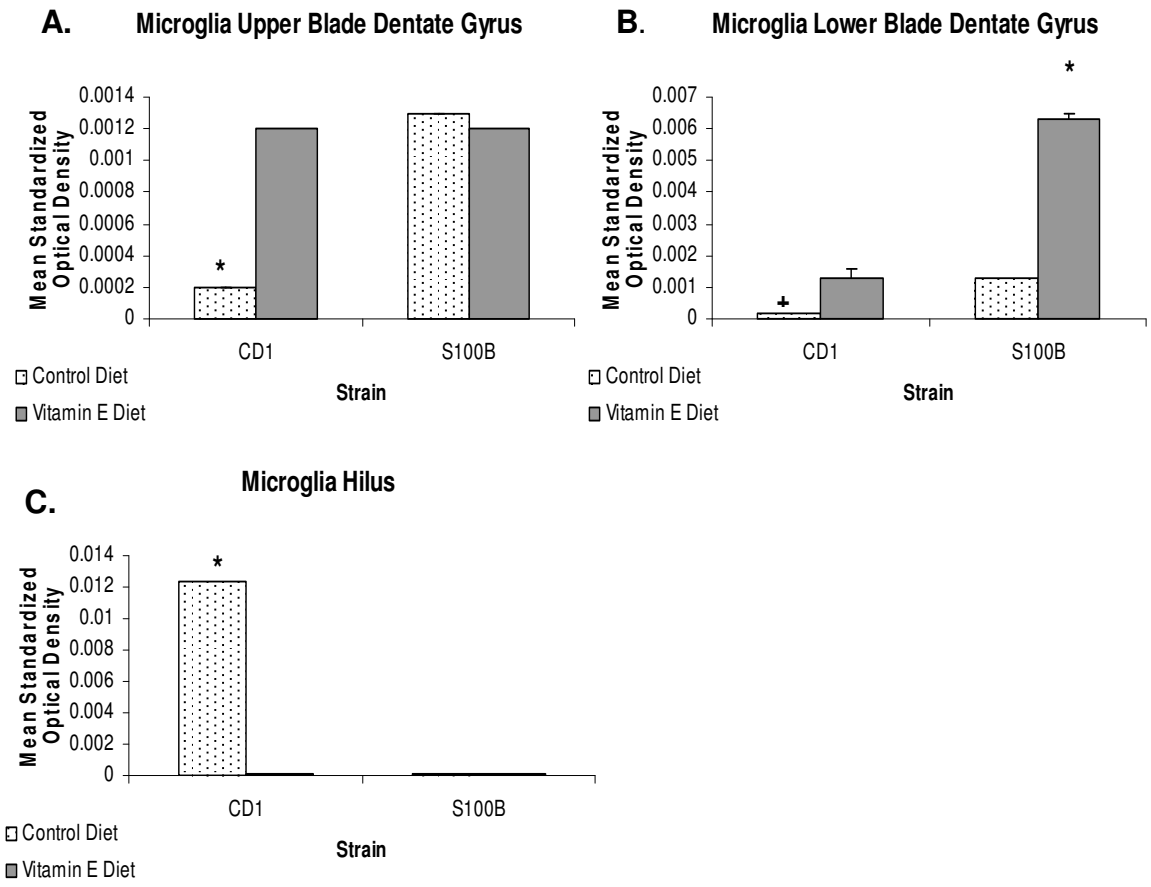

Figure 23. Average F4/80 microglial immunodensity in upper blade (A), lower blade (B), and hilus (C) of the dentate gyrus. S100B Vitamin E animals had greater immunoreactivity of activated microglial cells (B) than all other groups in the lower blade, $*p < 0.01$. CD1 control diet animals had significantly less reactivity than all other groups within the upper blade (A), $*p < 0.01$ and lower blade (B), $+p < 0.05$ of the dentate gyrus. Within the hilus (C), CD1 control diet animals had greater reactivity $*p < 0.01$ appearing mostly in the resting morphology.

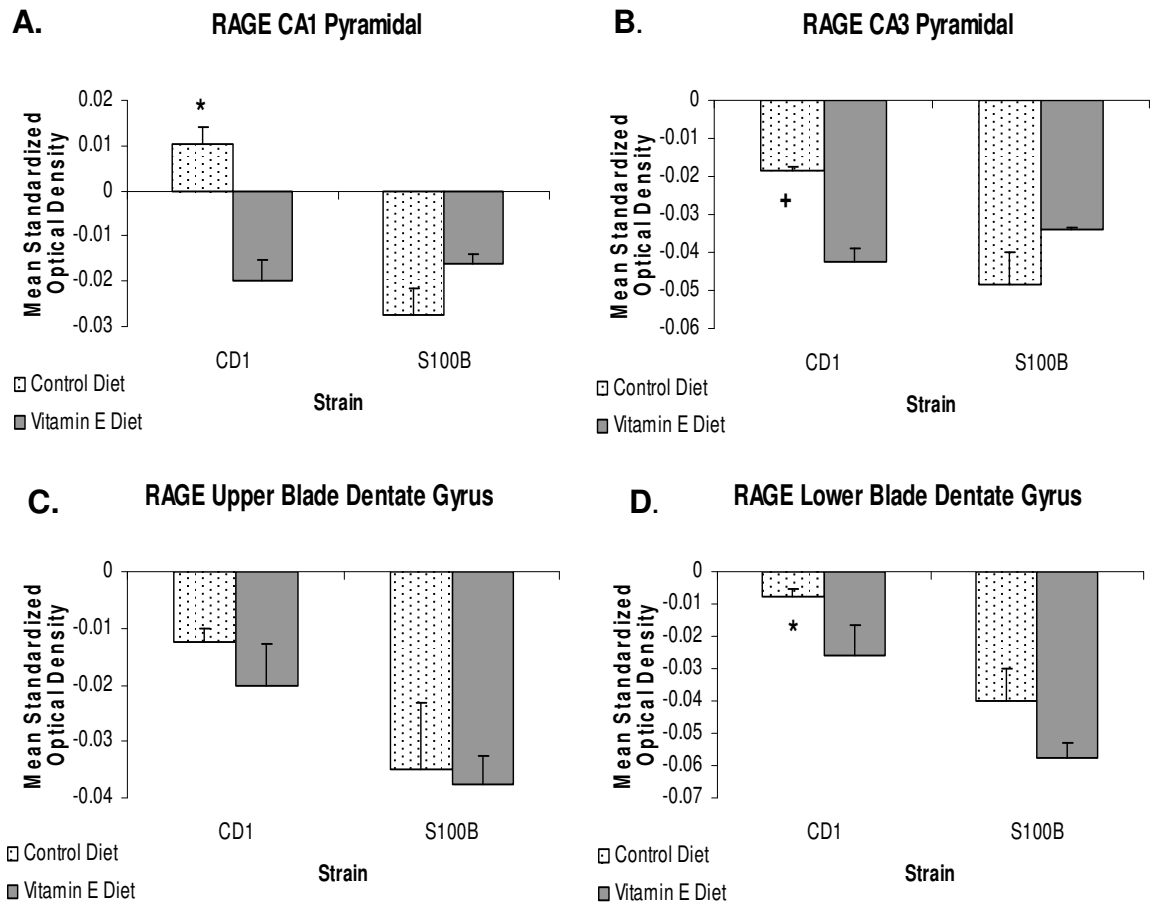

Figure 24. RAGE immunodensity in hippocampal CA1 pyramidal (A), CA3 pyramidal (B), upper blade (C) and lower blade (D) of the dentate gyrus. Within CA1 pyramidal (A), CD1 control diet animals had significantly greater RAGE expression than all other groups, $p < 0.01$. Within CA3 pyramidal (B), CD1 control animals had greater reactivity than CD1 Vitamin E and S100B control diet animals, $p < 0.05$. Within the lower blade (D), CD1 control diet animals had greater reactivity than S100B Vitamin E diet animals, $p < 0.01$.

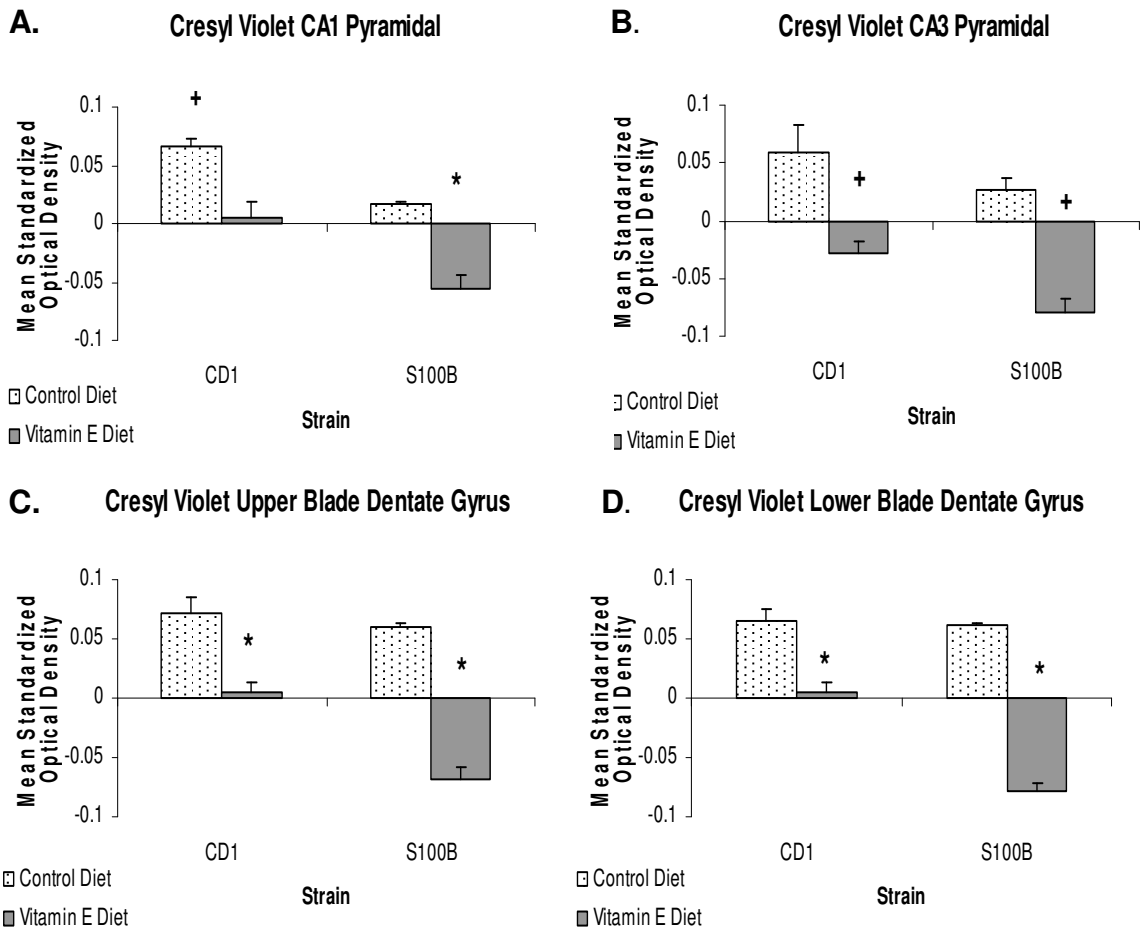

Figure 25. Cresyl violet neuronal density in hippocampal CA1 pyramidal (A), CA3 pyramidal (B), upper blade (C) and lower blade (D) of the dentate gyrus. Within CA1 pyramidal (A), S100B Vitamin E diet animals had significantly less neuronal density than all other groups, $p < 0.01$ while CD1 control diet animals had greater density than CD1 Vitamin E diet mice, $p < 0.05$. CA3 pyramidal (B) followed similar pattern with less neuronal density in S100B Vitamin E than all other groups and less neuronal density in CD1 Vitamin E as compared to control diet animals, $p < 0.05$. Within the blades of the dentate gyrus (C, D), S100B Vitamin E animals had significantly less neuronal density than all other groups while CD1 Vitamin E has decreased density as compared to CD1 and S100B control diet animals, $p < 0.01$